H2020-LCE-2016-2017

EUROPEAN COMMISSION

Innovation and Networks Executive Agency

Grant agreement no. 774392

E-LOBSTER

Electric losses balancing through integrated storage and power electronics towards increased synergy between railways and electricity distribution networks

Deliverable D1.1
Measures for energy losses prevention in the traction chain

Document Details

Due date	31.05.2019
Actual delivery date	31.05.2019
Lead Contractor	University of Birmingham
Version	Final rev0
Prepared by	University of Birmingham
Input from	FFE, RSSB
Reviewed by	RINA Consulting
Dissemination Level	Public

Project Contractual Details

Project Title	Electric losses balancing through integrated storage and power electronics towards increased synergy between railways and electricity distribution networks
Project Acronym	E-LOBSTER
Grant Agreement No.	774392
Project Start Date	01-06-2018
Project End Date	30-11-2021
Duration	42 months

The project has received funding from the European Union's Horizon 2020 research and innovation programme under Grant Agreement No 774392.

Table of Contents

Terms and abbreviations

The table below lists (alphabetically) the terms and abbreviations used in this document.

Abbreviation	Description
SOP	Soft Open Point
TPSS	Traction Power Substation
DPTS	Driver Practical Training System
GA	Genetic Algorithm
ATO	Automatic Train Operation

1 Introduction

The main objective of the E-LOBSTER project is to develop and demonstrate in relevant environment (a real underground railway in Madrid connected to a local power distribution network with a high penetration of RES) an innovative, economically viable and easily replicable Electric Transport-Grid Inter-Connection System. By properly managing the integrated system, it will be possible to establish mutual synergies between power distribution networks, electrified urban transport networks (metro, trams, light railways etc.) and charging stations for electric vehicles.

This report demonstrates the measures for energy losses prevention in the traction chain. The optimisation of the traction chain requires a detailed analysis of energy loss due to the each individual component of the traction system. This study will look separately at the contribution of the energy losses of the traction system, the electrical and friction braking, and also to the energy consumption of auxiliaries, including the cooling of traction motors and converters, the heating, venting and air conditioning (HVAC) system and the air compressors. In order to highlight the parts of the system mainly responsible for energy loss, different operating scenarios will be numerically simulated using the proposed modelling tool. Typical traction cycles with accelerations, coasting, braking and waiting times at the station will be simulated and the loss of the different components will be separately cumulated to understand their share at the end of the cycle.

This report first reviews the feeding architecture of electric railway systems, and then illustrates the energy flow within the railway network. The simulation tools to study the energy flow of railway network are introduced in this report. Based on the simulation tools, the power and energy performance of Metro de Madrid Line 2 and Line 12 with various operation strategies are studied. The methods to reduce energy losses for railway systems are finally analysed.

2 Connection of railways to the electric power infrastructure

2.1 AC railways

2.1.1 25 kV 50 Hz

Normally, the incoming feed of AC 25 kV railways is supplied from 132/275/400 kV grid networks. Connections to the public grid at feeding locations are typically 40 km to 100 km apart depending on the detail of the connections to the overhead contact line of the railway. Grid connections are single phase, and adjacent sections may be fed from different phase-pairs to reduce to impact of unbalanced single phase current. At the railway feeder stations, two incoming circuits are normally made available. Both of the feeds are capable of individually carrying the total traction load under normal traffic conditions, this will provide a power supply with a high degree of security. Figure 2-1 describes a typical feeding connection of 25 kV railway. Occasional connections for low voltage equipment such as signals are from the 25 kV line, but generally are from the local public supply directly. Stations and other locations fed from the local public supply.

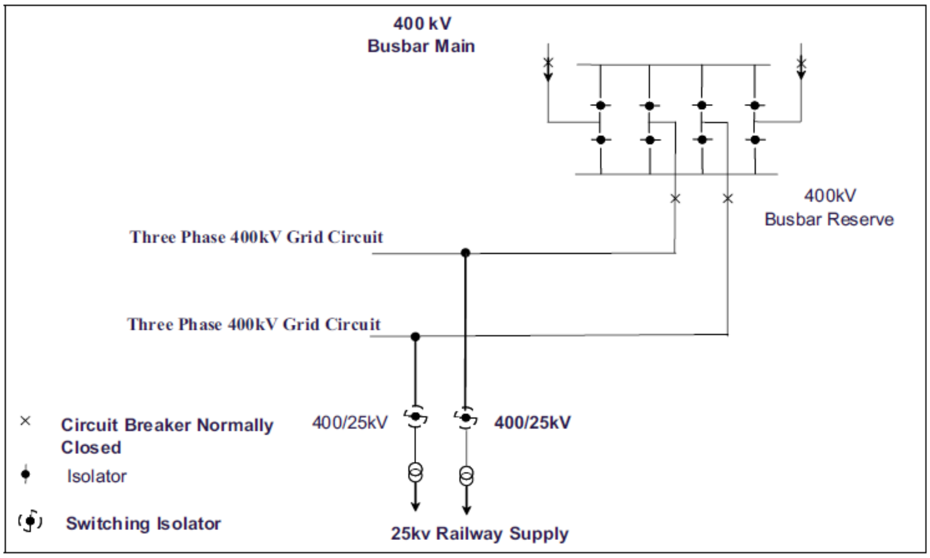

Figure 2-1 Typical Supply Feeding Arrangement for a 25kV Electrified Railway [1]

2.1.2 15 kV 16 2/3 Hz

This AC system is connected more like a DC system with all overhead contact lines connected together in parallel, and between feeding sections. Power is supplied from private generating stations (with a few converter stations to the public grid), through an extensive network of single-phase feeder circuits owned by the railway, at both traction voltage and higher transmission voltages. Stations and other locations fed from the local public supply.

[1] R. D. White, "AC 25kV 50 Hz electrification supply design," in 5th IET Professional Development Course on Railway Electrification Infrastructure and Systems (REIS 2011), 2011, pp. 92-130.

2.2 DC railways

2.2.1 DC Metro Railways

In modern railways, the DC traction substations are normally equipped with transformers and rectifiers, drawing electricity from local distribution networks. Figure 2-2 presents a typical feeding network for a DC railway system. The electrical supply fed to railways is typically at 132, 66 or 33 kV AC, depending on the size and demand of railway systems. A medium voltage distribution network is normally at 33, 20 or 11 kV, fed by step down transformers. The medium voltage network provides energy for the whole railway system. The passenger station is supplied by 415 V 3-phase transformed from 11 kV for domestic usage. Traction substations use transformers and rectifiers to convert 11 kV AC into 600 to 3000 V DC.

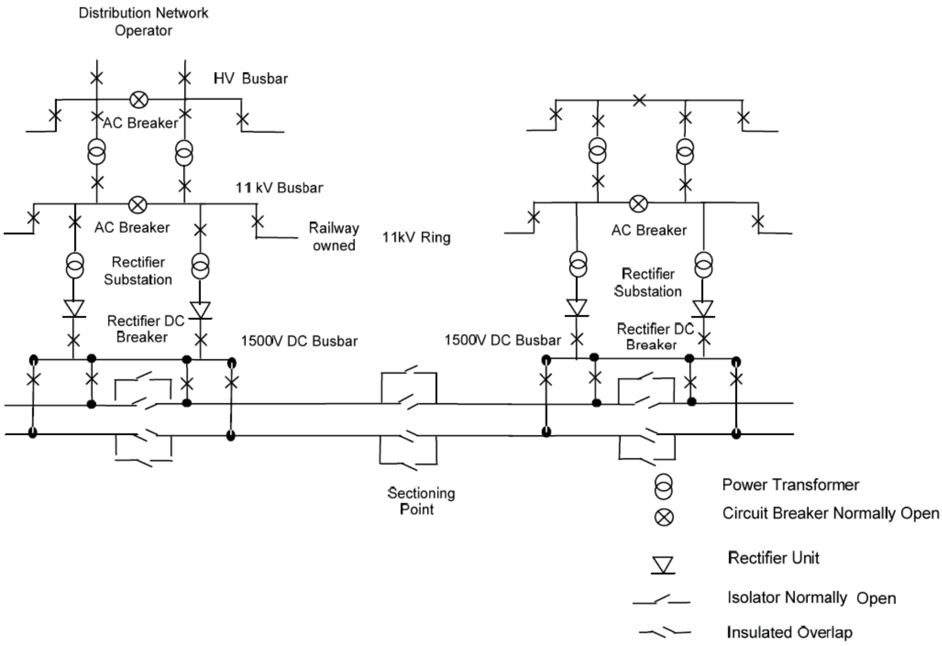

Figure 2-2 A typical DC feeding arrangement [2]

The traction supply for low voltage metro style railways typically employs low level conductor rail, and normally operates at nominal voltages of 600 – 750 V, supplied from Traction Substations alongside the route. To deliver the power demanded by a metro style railway, the current that needs to be delivered is in the order of 4500 A per train, and the distance that this current can be delivered is constrained by the resistance of the conductor rail. Traction Substations are therefore located alongside the line at intervals of 8-10 km. At track level substations operate in parallel, although the railway may be sectionalised to localise faults. Some railways use a return through the running rails, others have a fully insulated return system.

Whilst each traction substation could be connected to a local lower voltage (11 kV) public grid network as it is common in tramway practice, the magnitude and variability of the traction load of a

[2] R. D. White, "DC electrification supply system design," in 7th IET Professional Development Course on Railway Electrification Infrastructure and Systems (REIS 2015), 2015, pp. 1-29.

metro railway is such that connection to the public must be at a higher voltage level (132 kV or 400 kV). Connections to the public grid are therefore made at “Bulk Supply Points” and then distributed to the traction substations at a “distribution” voltage level. A general characteristic of these connections is that each traction substation can be connected through alternative connections with at least dual redundancy. Bulk supply points are normally provided with redundancy and divers supply connections. The extent to which connections are diverse and duplicated depends upon the risk of the loss of supply to the railway. An underground railway is normally supplied in a more robust, and correspondingly more costly manner, than surface level railway reflecting relative nature of the risks of the railway.

The DC railway in the south of England is generally above ground, and extends over a considerable distance, from London to the South Coast. The substations along this railway are generally fed from a linear distribution system operating at 33 kV supplied from “Bulk Supply Points” at each end of the distribution system. To avoid connecting diverse parts of the public grid through the railway distributions system an “open point” is maintained in the connection, but the system can be reconfigured to feed substations from alternate “Bulk Supply Points”. As a surface level railway, auxiliary loads are relatively low and can either be fed from a local traction substation, or a direct connection to the public supply. In this network there is little connection between the traction supply and auxiliary loads.

The London Underground as a more complex, relatively dense and extremely busy system with many deep level railway lines takes an approach based upon a desire to operate it safely and reliably even under partial failure conditions. The system is designed with multiple redundancy to maintain full services for single point failures throughout the system, and in the event of larger failures to enable safe evacuation of passengers, and preservation of infrastructure.

The underground takes a “private” supply from the “grid” at a number of points on the “public” power system through a series of “Bulk Supply Points”. The configuration can be altered to ensure supply is maintained to the whole railway, but not are electrically interconnected. In this system, a private generating station is also connected of sufficient size to be used for the economic reduction of peak loading of the grid connections, and to provide an emergency supply in the event of a major power outage.

From the “Bulk Supply Points” power is distributed through a 22 kV cable network to distribution points and traction substations, and further distributed to other traction substations at 11 kV. Low voltage 415 V three phase supplies to stations are obtained from adjacent substations by cable connection at smaller stations, but larger stations have dedicated high voltage to low voltage transformer rooms.

Further supplies are obtained from the local public “distribution” supply at each station to give a diversity of power supply for emergency lighting. To maintain emergency lighting in the event of loss of the main “grid” supplies and local “distribution” supplies, most stations also have some form of battery supply to maintain lighting to evacuate the station.

Signalling supplies are obtained on a dual redundant basis from adjoining traction substations. Both of these examples have an historic background of being originally supplied from railway owned generating stations prior to the widespread establishment of a local grid. Railways built or electrified in more recent times are likely to be more diverse incorporating a combination of connections to a strong “public grid” with a more limited number of railway owned cable connections.

High power DC systems (1.5 kV and 3 kV) that utilise overhead contact lines to supply the power to trains. In high-density areas, the current carrying capacity is increased by the use of twin contact wire and twin catenary wire and sometimes, additional parallel feeder wires. Traction substations are connected to the three-phase public grid at intervals of 15 km to 20 km. There may also be some railway owned feeding network for historical reasons, where local grid connections are sparse.

3 Configuration and Energy flows in DC railway systems

The typical energy flow diagram through the DC-fed railway is shown in Figure 3-1. There are three layers, namely substation level, catenary system level and train level. The substations collect electricity from the national electricity grid to feed the whole railway system.

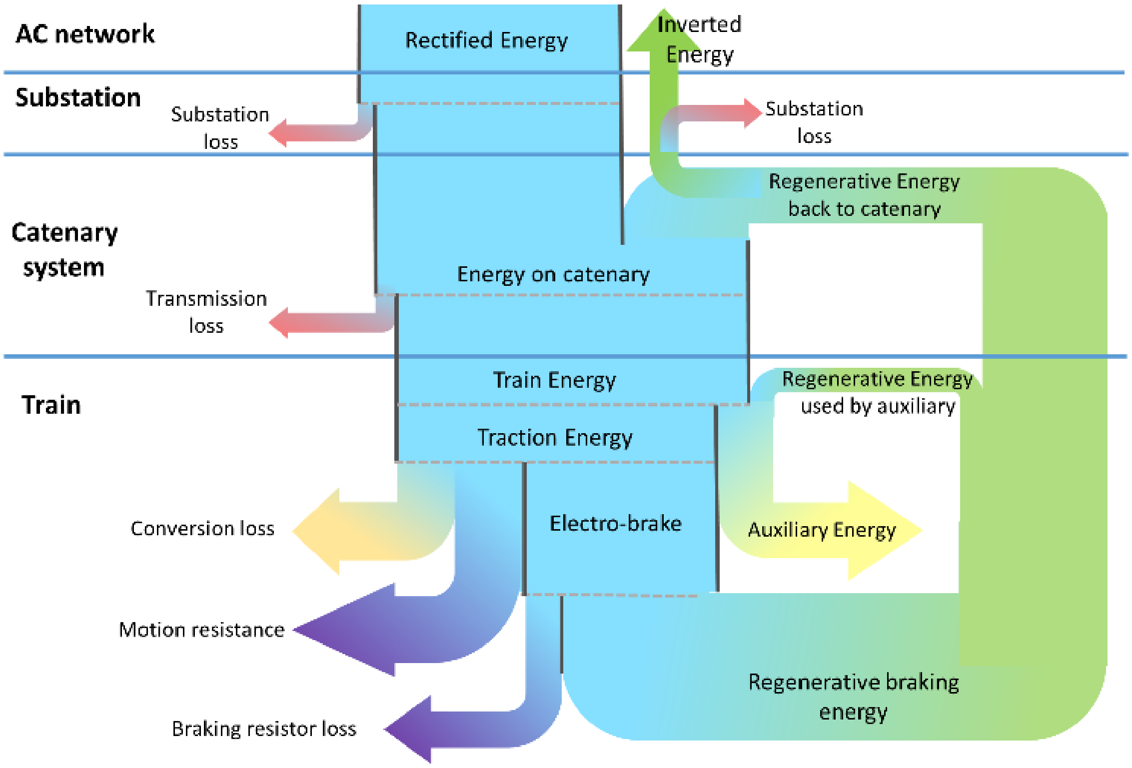

Figure 3-1 Typical traction energy flow in urban rail systems[3]

The substation energy is the bill paid by the railway operators. From the load flow analysis, the voltage and current of each substation can be obtained. The substation energy consumption is computed by integrating all substation instantaneous power over the train operation time.

Due to the internal resistance of substations, some energy will be dissipated inside the substations as heat. The electrical losses within each substation are determined by the losses in the transformer and diodes.

After the losses from substations, the rest of the substation energy can be transferred to the catenary. The energy on the catenary combines some of the substation energy and the regenerative braking energy, which is transferred back to the catenary system. As the current goes through the resistive transmission lines, some energy is dissipated as heat (transmission loss).

Trains receive the electricity from pantographs, which connect with the transmission lines. The train power depends on the voltage and current at the pantograph, which is solved by a load flow solver. Thus, the train energy can be computed by integrating all train instantaneous power over the time.

[3] Z. Tian, G. Zhang, N. Zhao, S. Hillmansen, P. Tricoli and C. Roberts, "Energy Evaluation for DC Railway Systems with Inverting Substations," 2018 IEEE International Conference on Electrical Systems for Aircraft, Railway, Ship Propulsion and Road Vehicles & International Transportation Electrification Conference (ESARS-ITEC), Nottingham, 2018, pp. 1-6.

The train energy and some of the regenerative braking energy are used for train traction and the auxiliary system.

The on-board auxiliary power is used to supply lights and air conditioners, etc. Therefore, the auxiliary energy consumption can be calculated by integrating the power of the on-board auxiliary system over the time.

When the train is braking, a small part of the regenerative braking energy is used by the on-board auxiliary system directly. This energy can be calculated by the overlapping of auxiliary power and electric braking power.

The train traction energy is the electricity consumed by the train for traction, which depends on driving styles. It is the sum of the mechanical energy at the wheels and the conversion loss. The mechanical energy at the wheels depends on the train tractive effort and train speed.

Some energy is dissipated by transforming from electrical to mechanical energy (conversion loss). The mechanical energy at the wheels is used to move the train and overcome the motion resistance. The rest of the mechanical energy is train kinetic energy consumption. This kinetic energy is not the maximum kinetic energy obtained by the train at running, but the part of the kinetic energy, which is dissipated by the braking system.

A blending of the electric and mechanical brake is commonly used in modern trains. Electric braking uses the traction motor as a generator to regenerate braking energy. Friction braking is used when the motor cannot provide sufficient braking effort. Therefore, part of the kinetic energy of the train is dissipated by friction braking. The rest of it is converted into electricity by electric braking with some loss of energy in the mechanical to electrical conversion.

Most trains with regenerative braking are also fitted with braking resistors in case the regenerative energy is not receptive. The regenerative braking energy equals the electric braking energy subtracted by the energy dissipated by the braking resistor. Part of the regenerated energy is used by the on-board auxiliary system directly and the rest of the regenerated energy flows back to the catenary system. The regenerative energy fed back to the network can be used by other trains in the network or be inverted to AC to supply AC network.

4 Simulation tools for the analysis of energy losses

4.1 Single-train simulator

Figure 4-1 indicates the forces on a traction vehicle located on an uphill section of track. The tractive effort (*F*) applied to a vehicle is used for moving the train against the friction forces (*R*) and gravitational forces ($Mg\sin(\alpha)$) in moving the mass of the train uphill.

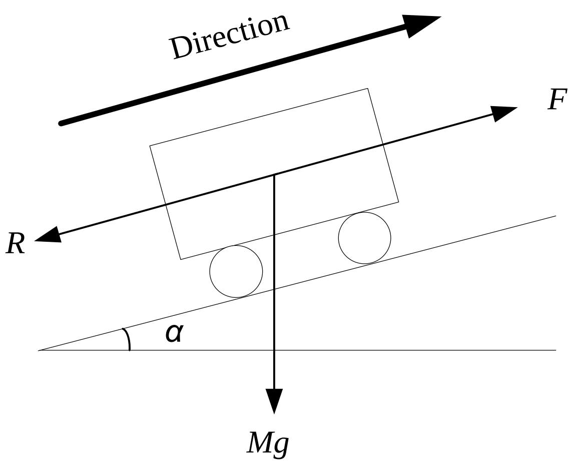

Figure 4-1 Forces on a traction vehicle

The train movement can be determined by standard Newtonian equations of motion. In the longitudinal direction, the motion of the vehicle is governed by the tractive effort, the gradient and the vehicle resistance, known as Lomonossoff's equation in (4.1).

$$M_e \frac{\mathrm{d}^2 s}{\mathrm{d}t^2} = F - Mg\sin(\alpha) - R \tag{4.1}$$

Train driving control can be generally categorised into four modes: motoring, cruising, coasting and braking. The train speed trajectory can be generated by different driving strategies. Figure 4-2 shows an example of a speed curve with these four modes in sequence.

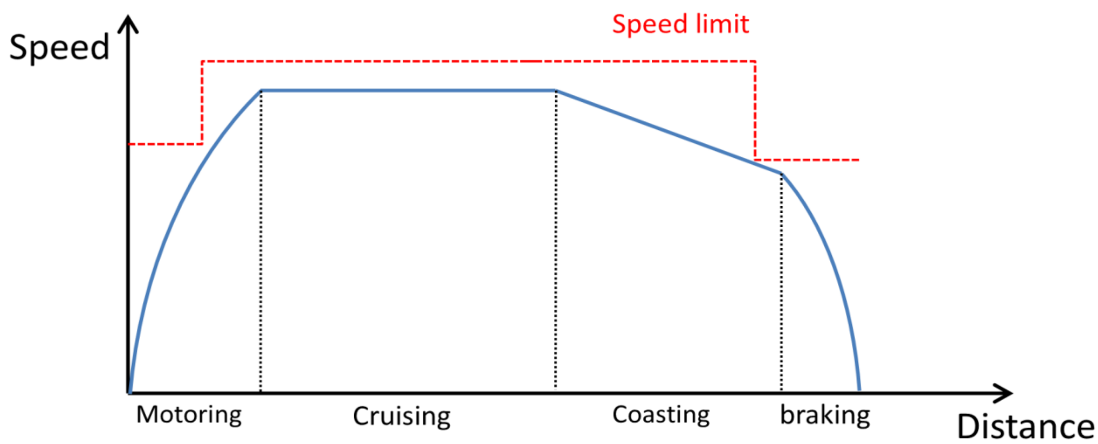

Figure 4-2 An example of a train speed trajectory

A single-train movement is modelled based on the vehicle characteristic and route data. The vehicle characteristic includes vehicle mass, tractive effort parameters and Davis constants. The route data includes gradient, speed limits and station positions along the route. Figure 4-3 describes the structure of the motion simulator. The driving strategies are treated as dynamic inputs to the single-train motion simulator. The simulator outputs the train speed profile based on the driving styles and fixed inputs. The train power requirement and traction energy consumption can also be computed for further studies.

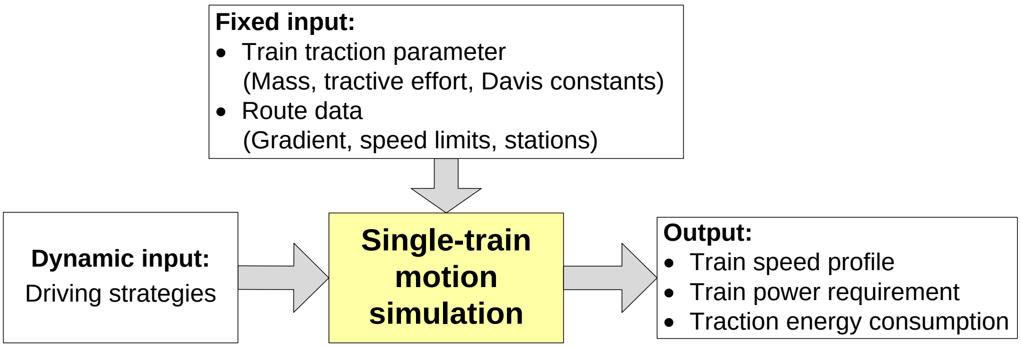

Figure 4-3 Diagram of motion simulator structure

A time-based simulator can be developed using the structure above. A whole journey is discretised in time, and then it becomes a combination of vehicle state at each time step. Figure 4-4 describes an example of the movement of a vehicle. The relationship between distance and time as well as the relation between speed and time can be found in this figure. The time interval is expressed by ΔT. The time step with 1 second is proper for energy evaluation, which is used in this thesis. The driving controls are a sequence of tractive effort values at each time step. The tractive effort is assumed as a constant during each time interval. The state of the vehicle including acceleration, speed, position and power can be calculated according to the driving controls at each time step.

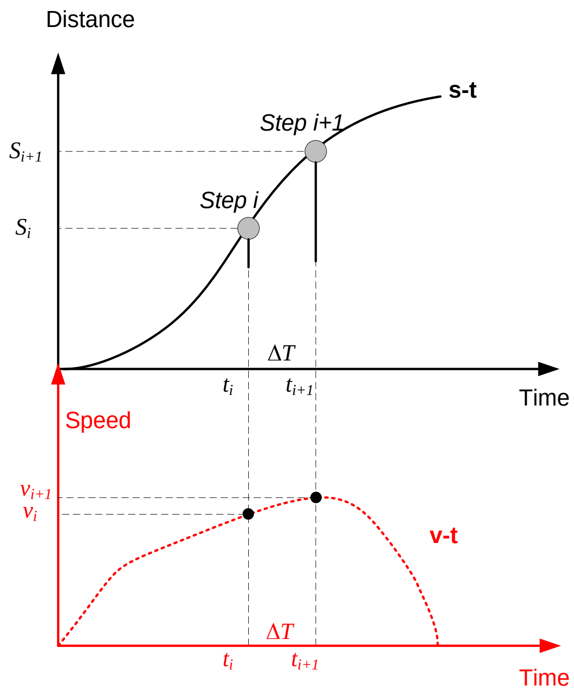

Figure 4-4 Vehicle state switch

4.2 Multi-train simulator

In a DC railway power network, the traction rectifier substations are the primary electricity source for vehicles. Figure 4-5 presents a typical DC traction power network with multiple trains on up and down tracks. The rectifier substation is connected to the DC busbar, which feeds the power network in both the up and down tracks. When the transmission line voltage is higher than the substation voltage itself, the rectifier substation will prevent current from flowing back to the AC utility grid.

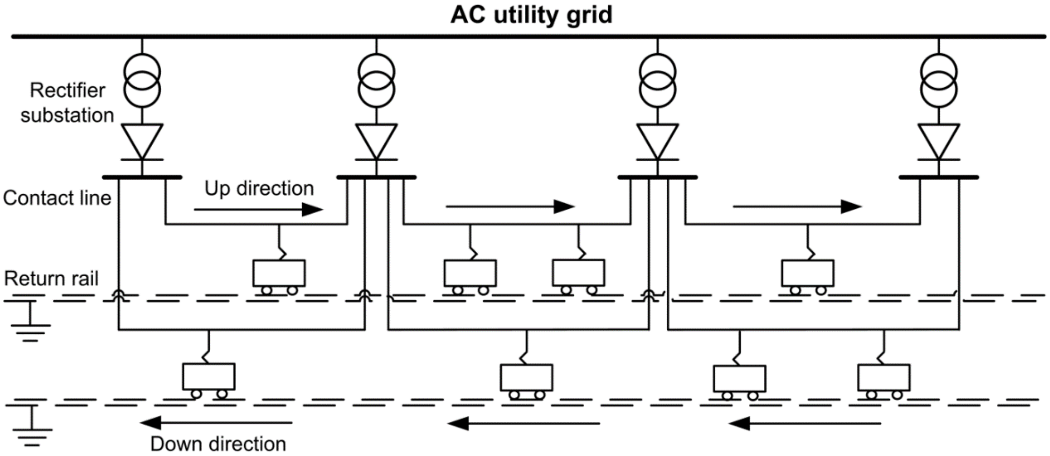

Figure 4-5 Typical DC traction power network

Generally, the whole DC traction power system of a single metro line is made up of a single electrical network to minimise the power transmission losses and maximise the receptivity for regenerated energy. An equivalent circuit of a DC railway power network to compute substation energy consumption and regenerative braking energy is shown in Figure 4-6. The train is presented as dynamic power unit, which is considered as power load when the train is motoring or power source when the train is braking. In Figure 4-6, the current source with current flowing to return rail is motoring train, while that with current back to contact line is braking train. The rectifier substation can be simplified as an ideal voltage source in series with an equivalent source resistance and a diode. The diode is used to rectify the AC into DC, and also results in blocking reverse current when the transmission line voltage level is higher than substation open circuit voltage due to a large regenerative braking power. Therefore the current comes from substations has to be positive. The power conductors (including the contact line and return rail) are modelled with resistances proportional to the conductor length. The train, substation and track-paralleling hut split the conductor model into two resistances.

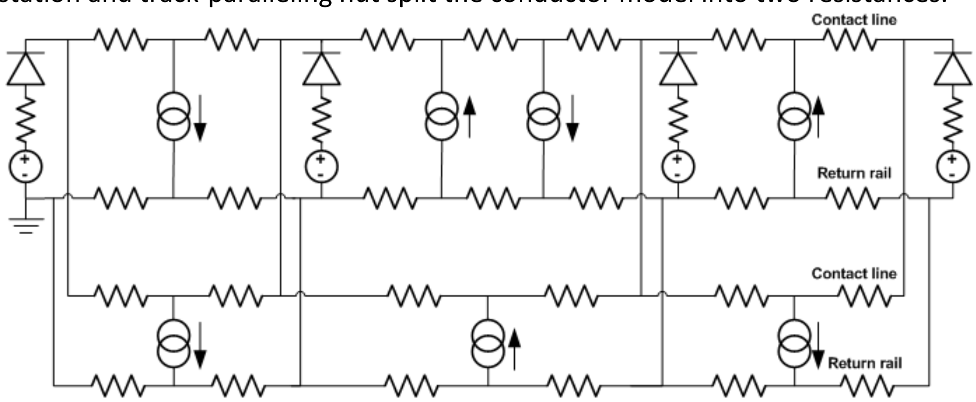

Figure 4-6 DC traction power network equivalent circuit

The electrical power requirement for each train has been calculated based on the movement simulation. Thus, the train voltage and current are simply related to the electrical power at the train by

$$P_{elec\_n}(t) = V_n(t) \times I_n(t) \tag{4.2}$$

From the network circuit, the nodal analysis can be expressed in matrix form.

$$[I] = [Y] \times [V] \tag{4.3}$$

The resulting nonlinear equations are solved using the improved bi-factorization iterative algorithm. In this paper, both overvoltage regenerative braking and under voltage protection are also considered. Not all of braking energy can be transferred to overhead line as regenerative energy if the voltage would become too high. The actual train power should be computed by the results of nodal analysis.

A Multi-Train Energy Simulator (MTES) has been developed to evaluate the energy flow in a railway system. The structure of the MTES is shown in Figure 4-7. This simulator combines single-train motion simulation and multi-train power network simulation. The dynamical input parameters (driving strategies) with fixed input (traction and route data) are imported into the motion simulator. Then, the output single train trajectory and power requirement with a whole-day timetable and power network parameters are imported into the power network simulator, which will export the electrical energy consumption, including substation and transmission losses, as well as the actual used and wasted regenerative energy. According to the energy evaluation results from the multi-train power network simulation, the dynamic inputs (driving strategies and timetable) can be modified to optimise the total energy consumption.

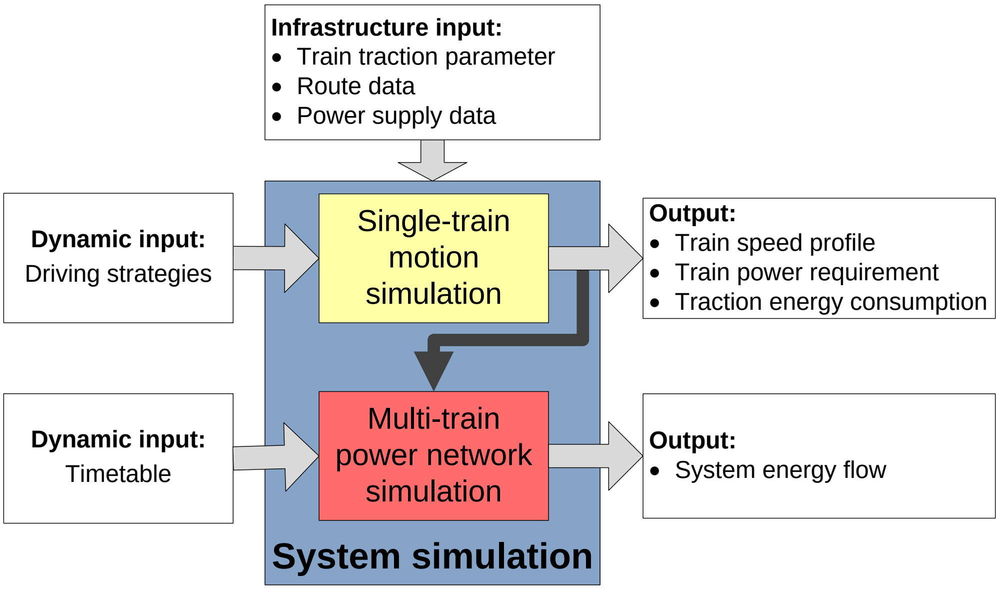

Figure 4-7 Diagram of MTES structure

5 Analysis of energy losses for DC railway systems

5.1 Train auxiliary losses

The aim of the following section is to provide a general description of the different auxiliary losses that may take place within the facility that is under study. Therefore, it is focussed on four types of devices: the cooling system of traction motors, HVAC (heating, venting and air-conditioning), air compressors and station losses.

The structure that is going to be followed to go through each of them would be, firstly, the sort of technology used and, secondly, a rough calculation of the amount of power losses that it reaches.

In order to get the big picture of the system, the following figure may simplify the whole system functioning helping to understand it.

Figure 5-1 General picture of the studied system[4]

5.1.1 Cooling of traction motors and converters

Power losses in traction motors, or electrical motors in general, are well known and theoretically easy to calculate. As the aim of this section is to calculate the power losses due to motor cooling, it is important to set the knowledge base of the temperature increase in traction motors.

Electrical motors are electrical machines whose functioning is based on electromagnetic laws. They are basically formed by two main parts: the rotor and the stator. Both are surrounded by a set of bobbins, which are paired and that are called poles.

The functioning of the system is based on Faraday and Maxwell electromagnetic laws. Therefore, AC current flows through the bobbins of the stator, creating a sinusoidal magnetic field, which induce an electrical current into the set of bobbins of the rotor. The interaction between the magnetic field and the electrical current causes a torque in the rotor and this allows the motor to spin and generate mechanical power.

[4] Recovered from: https://www.howden.com/en-gb/industries/transportation/industrial-fans-for-railways

These fields and the interaction between the rotor and the mechanical load cause the main power losses in traction motors. There are three main factors:

- Cupper losses: this refers to resistive losses due to current flowing through the circuit of the set of bobbins in the stator and the rotor.
- Iron losses: this refers to magnetic losses due to the magnetization of the stator.
- Mechanical losses: this refers to losses due to the friction in the motor axis and the cooling system.

These losses, which cause a temperature increase in the motor, may be calculated with some parameters that should be supplied by the manufacturer.
Consequently, traction motors, and also converters, are affected by a decrease in their efficiency due to an increase of the working temperature caused by different factors. In the case of the traction motor, the increase of temperature over the nominal temperature has three main consequences to be considered:

- Increase in ageing effects and deterioration within some essential components.
- Decrease of the remanence and coercivity of magnets that may lead to partial or full demagnetization.
- Increase of the resistivity of winding conductors.
- Geometrical variation of the motor structure.

In order to avoid these issues, cooling systems are mandatory in traction motors. There are mainly two kinds of cooling systems: active and passive. The idea is to use an external fluid (gas or liquid) in contact with the surface of the traction motor, generating a rather thin film that allows transferring the heat from the motor to the fluid, decreasing the temperature of the first one and increasing the temperature of the second one, which cools down later. In order to achieve a better understanding of the parameters that affect the cooling of the motor, the formula that leads the convection effect is:

$$dQ = h \cdot dA_s \cdot (T_s - T_f)$$

This formula introduces the parameters that rule the amount of heat flux that the cooling system is able to dissipate. At the next table, the influence of some parameters may be observable.

Cooling method		σ, kPa	A_t, kA/mm^2	J, A/mm^2	$h, W/mm^2K$
Natural convection		-	-	1.5-5	5-30
Forced gas cooled	Air	<15	<80	5-10	20-300
	Hydrogen	<25	70-110	7-12	100-1000
Forced liquid cooled	Indirect	20-60	90-130	7-20	100-1000
	Direct	60-100	100-200	10-30	200-25000
	Phase change	-	-	-	500-50000

Table 5-1 Typical values for different cooling methods

Once all the principles have been explained, the different types of cooling technologies that usually apply to traction motors are going to be shown, also trying to estimate interesting data that may lead to a rough calculation of power losses.
The first kind of active cooling that is considered, is achieved using air or another gas. To do so, the air must be forced to move by a fan. This technology has two branches, depending on the way that the cooling circuit is build: EFC (enclosed fan cooled) and OFC (open fan cooled). In the first one, the internal circuit (inside the traction motor) is isolated form the external one, using two fans for each

circuit, whereas in the second one the circuit is not re-circulated and the gas flows from out of the motor to the inside. The functioning is shown in the next figures.[5]

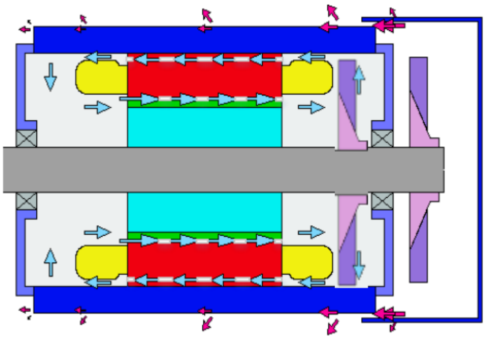

Figure 5-2 Structure of an EFC motor

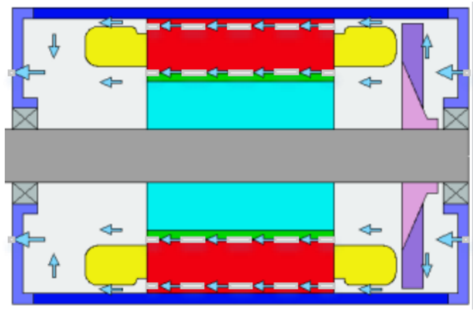

Figure 5-3 Structure of an OFC motor

As the goal of this text is to try to give the basis for a calculus of the power losses in the cooling of the motor, the losses in the fan are shown in the following figure.

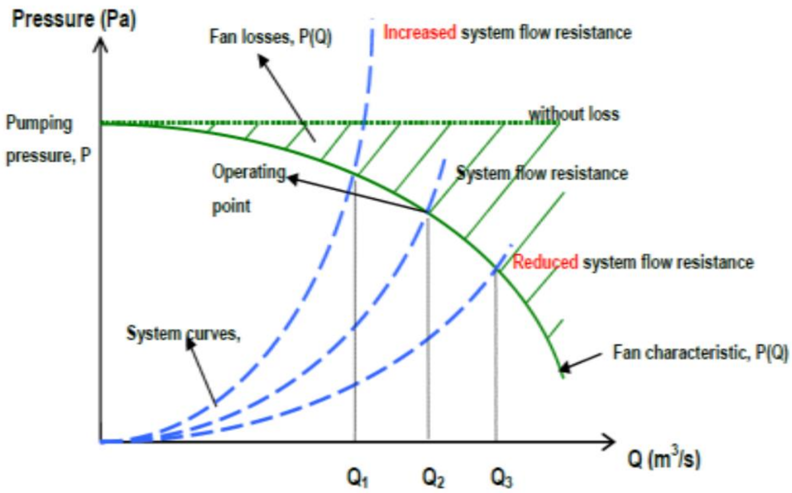

Figure 5-4 Typical power losses of a fan[6]

The next kind of active cooling that is considered uses a liquid as coolant, which is more powerful regarding the cooling capacity. Power losses referred to this kind of cooling would be those that are used to run the pump.

Once these principles and main technologies used nowadays have been introduced, it is possible to tackle a rough calculation of the power losses in the cooling system. As far as the aim of this study is to calculate the power loss in the motor cooling system, the most important element to focus on is the fan or the pump that propel the fluid. As it can be checked in many companies that are specialized in railway cooling systems, air-cooling are more used in motor traction systems.

A proper approximation to actual or logical values of power loss may be reached following two different paths.

---

[5] Yaohui Gai, Mohammad Kimiabeigi, Yew Chuan Chong, James D. Widmer, Xu Deng, Mircea Popescu, Fellow, IEEE, James Goss, Member, IEEE, Dave Staton, Member, IEEE, and Andrew Steven . Cooling of Automotive Traction Motors: Schemes, Examples and Computation Methods– A Review

[6] Recovered from: https://www.howden.com/en-gb/industries/transportation/industrial-fans-for-railways

The first one is more theoretical and it consists in comparing the heat transfer formula of convection with the energy formula as it follows.

$$dQ = h \cdot dA_s \cdot (T_s - T_f) \rightarrow Q = P = h \cdot A_s \cdot (T_s - T_f) = \dot{m} \cdot C_s \cdot \Delta T$$

$$\dot{V} = \frac{\dot{m}}{\rho}$$

Considering that $\dot{V}$ represents the air volume flow that is propelled by the fan, the power of the fan required to propel the airflow may be calculated, once the heat to be dissipated is known.
The second one, which is more practical and rather more accurate, is to contact a supplier, who provides the technical data of the fan and, therefore, the power that the cooling fan requires.
All these concepts and calculation methods that has been applied to traction motors may also apply to converters systems.

5.1.2 Heating, venting and air-conditioning (HVAC) system

Heating, venting or ventilation and air-conditioning (HVAC) systems are rather important in order to fulfil the quality and comfort requirements that current railway systems demand. Besides, these systems are also important to be taken into consideration regarding power losses, as, according some studies, these account for up 30% of the overall energy demand.
It is important to notice the inputs that affect HVAC railway system in order to avoid unnecessary power losses and to design more efficient systems. It is also imperative to be aware that these power losses are rather variable due to the wide range of thermal loads that affect rolling stock. For instance, thermal loads within the vehicle, changing meteorological parameters or different operation profiles of a train. Within these examples, some of them cause slow variations (e.g. ambient temperature) and other cause quick changes in the temperature inside the rolling stock (e.g. solar radiation, doors opening). . The following figure illustrates these examples.

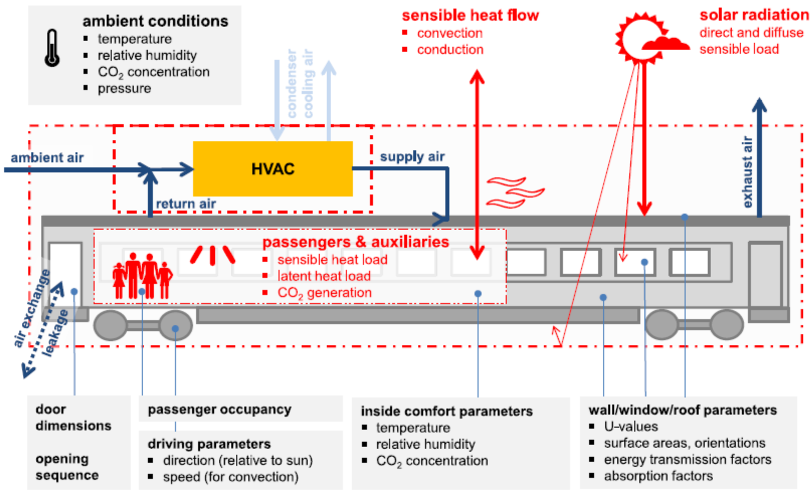

Figure 5-5 Thermal loads diagram in a HVAC system[7]

Power losses that belong to these systems are, in principle, easier to calculate due to the standards, papers and information supplied by several companies that work in this sector. Besides, there also

[7] C. Luger, J. Kallinovsky, R. Rieberer Identification of representative operating conditions of HVAC systems in passenger rail vehicles based on sampling virtual train trips

some studies that try to simulate power losses in HVAC systems in order to check the influence of different parameters.[8]

Making use of the standard parameters that affect HVAC systems, it is possible to roughly measure the air flow that is coming in and out the rolling stock, taking into consideration the maximum and minimum permissible temperatures and the minimum flow of venting air. However, as one said before, the variability between different facilities is an important aspect to consider. The following tables have been taken from the standards EN 13129-1 and EN 14750-1.

Zone	**Winter**	**Summer**		
	Minimum outside temperatures [℃]	Maximum outside temperatures [℃]	Relative humidity [%]	Equivalent solar radiation load $[W/m^2]$
I	-10	+40	40	800
II	-20	+35	50	700
III	-40	+28	45	600

Table 5-2 Design conditions[9]

Zone	**Winter**	**Summer**		
	Minimum outside temperatures [℃]	Maximum outside temperatures [℃]	Relative humidity [%]	Equivalent solar radiation load $[W/m^2]$
I	-15	+45	30	800
II	-25	+40	40	700
III	-45	+33	30	600

Table 5-3 Extreme conditions[10]

Outside temperature (T_{em}) [℃]	**Minimum frequency of ventilation equivalent to +20°C and 50& of humidity**
$\boldsymbol{T_{em} < -15}$	$10\ m^3/h \cdot viajero$
$\boldsymbol{-15 \leq T_{em} \leq -5}$	$15\ m^3/h \cdot viajero$
$\boldsymbol{-5 \leq T_{em} \leq +26}$	$20\ m^3/h \cdot viajero$
$\boldsymbol{T_{em} > +26}$	$15\ m^3/h \cdot viajero$

Table 5-4 Vehicles with air conditioning system[11]

It is also important to notice that the HVAC system is installed in different parts of the rolling stock (wagons, stairs, doors, engine driver cabin) that are affected by different boundary conditions.

---

[8] C. Luger, J. Kallinovsky, R. Rieberer Identification of representative operating conditions of HVAC systems in passenger rail vehicles based on sampling virtual train trips

[9] [4] [5]EN 13129-1 and EN 14750-1

Once the different parts of HVAC system and the aforementioned applicable standards, a method to be able to calculate the power requirements of this system is going to be summarized. The study[12] gives some inputs that are needed to be able to foresee the losses in HVAC system. It does not make sense to summarize the algorithm used in this study once this has been quoted. However, some of the inputs that are necessary to run the study are:

- Train trips and schedules
- Meteorological data
- Profile of passenger occupancy
- Vehicle parameters

To conclude this section and to justify why no estimated calculation has been provided, it is vital to notice the wide range of parameters and the variability of them that affect the HVAC system. Besides, HVAC losses, even if it is treated as the same system, depend on the function that the system is carrying out.

5.1.3 Air compressors

HVAC systems need a fluid in order to be able to heat, cool or ventilate the rolling stock, which is taken from the outside. The fluid that in this case is air, needs to be compressed and filtered in order to fulfil the requirements of the system. A thermal machine, which is called compressor, manages the compression of this fluid. The compression cycle is known and the study of it allows understanding and calculating the thermodynamic power losses.
As the aim of the text section is the understanding and calculation of the power losses of compressors, it is important to mention that there are two main sources: thermodynamic cycle and mechanical losses.
Thermodynamic cycle of a compressor responds to the next figure.

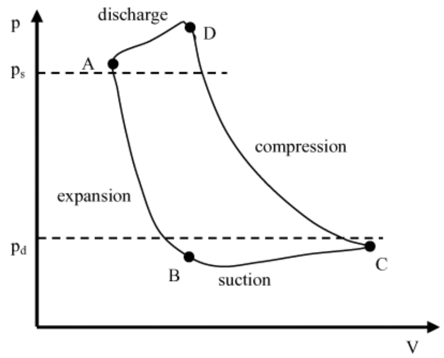

Figure 5-6 Thermodynamic compressor cycle

As it may be observed, the area within the input and output pressure (p_d, p_s) is the power actually used to compressed the fluid, whereas the area that lies above the p_s and under p_d represents discharge and suction losses due to the action of the valves.
Regarding the mechanical power losses, the friction of the piston or compressor paddles (depending on the system) causes a power loss that result in a temperature increase.

[12] C. Luger, J. Kallinovsky, R. Rieberer Identification of representative operating conditions of HVAC systems in passenger rail vehicles based on sampling virtual train trips

These power losses may be calculated taking into account the efficiency data of the compressor, provided by the manufacturer. So that, the efficiency of the compressors strongly depends on the technology that it works with. It is shown in the following table.

Compressor type	Efficiency
Centrifugal	0.70-0.85
High speed reciprocating	0.72-0.85
Low speed reciprocating	0.75-0.90
Rotary screw	0.65-0.75

Table 5-5 Efficiency of compressors regarding the type of technology[13]

Once the power of the compressor that is used and its efficiency is known, the power losses will be easier to estimate.

5.2 Train traction losses

The tractive energy consumption depends on the driving controls including cruising speed and coasting speed, as shown in equation (5.1), where f defines the relationship between the two driving controls and the traction energy consumption calculated using the simulator.

$$E_{traction} = f(v_{cr}, v_{co}) \tag{5.1}$$

Where:

- $E_{traction}$ is the train electrical traction energy consumption;
- v_{cr} is the cruising speed;
- v_{co} is the coasting speed.

The train running time is expressed in equation (5.2), where g represents the simulation process to calculate the train running time.

$$T = g(v_{cr}, v_{co}) \tag{5.2}$$

Where:

- T is the running time.

Train energy consumption can be traded off against running time. In theory, energy consumption is relatively reduced when running time increases. Figure 5-7 illustrates this formulation graphically. Each point in Figure 5-7 represents the energy consumption against running time resulted by a random driving control. The best driving operations with the lowest energy consumption for each second are shown in red, which constitute the bottom line of the driving results.

13 Campbell, J.M. (2014). Gas Conditioning and Processing, Volume 2: The Equipment Modules, 9th Edition

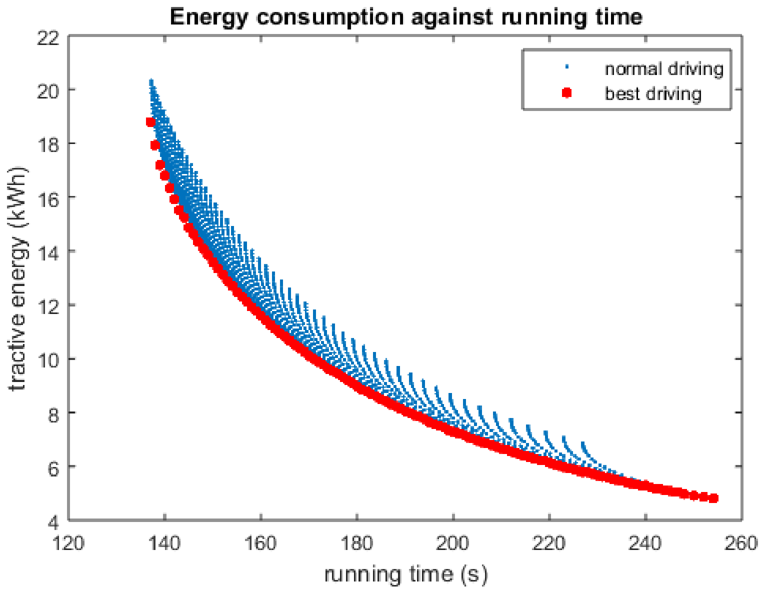

Figure 5-7 Result of energy consumption on running time

Train traction energy optimisation aims to reduce energy consumption within the running time constraints. An example of driving operations with three different driving patterns is shown in Figure 5-8. All three operations take the same running time but have different energy consumption costs. From the speed trajectory curves, the first driving cruises at the highest speed (80 km/h) and coasts until it reaches the lowest speed (48 km/h), while the third driving cruises at the lowest speed (66 km/h) and coasts until it reaches the highest speed (56 km/h). However, the second driving costs the lowest energy, followed by the first driving. The tractive energy profile shows the energy consumption during the running. As shown in Table 5-6, the first driving with a higher cruising speed costs more motion energy loss (5.95 kWh). This is because the high-speed running increases the motion resistance. With the same journey time, a high cruising speed leads to low coasting speed and late braking. Thus, the kinetic energy may be reduced, which is 1.91 kWh for the first driving. As for the third driving, the motion loss is lower, but the kinetic energy is higher resulting in the highest total tractive energy consumption. Therefore, a balance between cruising speed and coasting speed needs to be considered, and the best combination should be found.

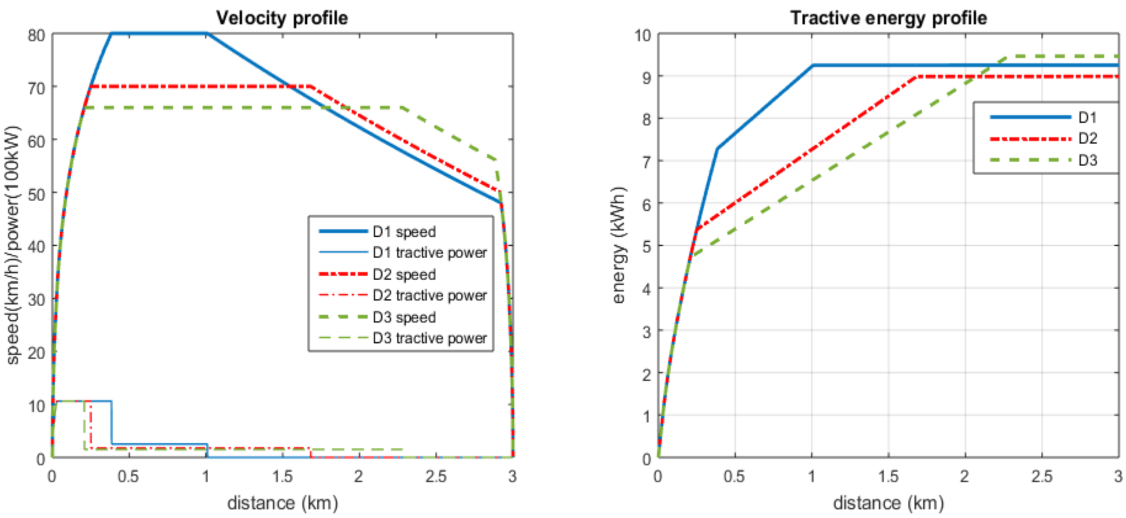

Figure 5-8 Speed and energy diagram of different driving patterns

Table 5-6 Results of different driving patterns

Driving pattern	D1	D2	D3
Distance (km)	3	3	3
Journey time (s)	180	180	180
Cruising speed (km/h)	80	70	66
Coasting speed (km/h)	48	50	56
Traction energy (kWh)	9.25	8.98	9.46
Traction loss (kWh)	1.39	1.35	1.42
Motion loss (kWh)	5.95	5.55	5.45
Kinetic energy (kWh)	1.91	2.08	2.59

5.3 Transmission and substation losses

5.3.1 Transmission losses

The energy on the catenary combines some of the substation energy and the regenerative braking energy which is transferred back to the catenary system. As the current goes through the resistive transmission lines, some energy is dissipated as heat. The energy loss in transmission is given in equation (5.3). The resistance of the transmission conductor is a time-varying variable, which is obtained according to the train locations and network.

$$E_{trans\_loss} = \int_0^T \sum_{n=1}^{N_c} (R_n(t) \times (I_n(t))^2)\, dt \tag{5.3}$$

Where:

- E_{trans_loss} is the transmission loss;
- N_c is the number of power transmission conductors;
- $R_n(t)$ is the resistance of a piece of transmission conductor at time t;
- $I_n(t)$ is the current of a piece of transmission conductor at time t.

5.3.2 Substation losses

DC-traction systems are preferred and extensively used in urban railways and suburban or mainline services like light and heavy metro trains. The most common DC-traction voltages for the respective systems are 600, 750, 1500, and 3000 V. The transformer-rectifier substations include usually uncontrolled rectifiers, whose pulse number is determined by the traction transformer windings and the static converter configuration. The common schemes are 6-pulse, 12-pulse, and even 24-pulse diode-based rectifiers. Figure 5-9 illustrates the simplified structures of the common DC-traction substations based on six-pulse and twelve-pulse parallel/series uncontrolled rectifiers and the associated waveforms of the phase voltages and currents.

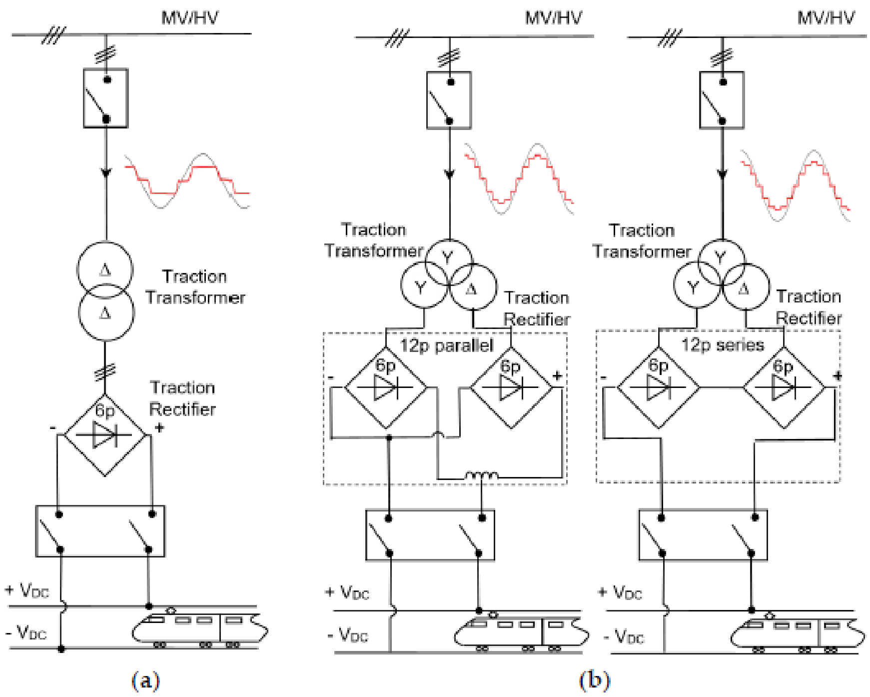

Figure 5-9 Simplified schemes of the usual DC-traction substations and specific waveforms of the supply phase current and voltage: (a) case of 6-pulse uncontrolled rectifier (b) case of 12-pulse parallel and series uncontrolled rectifier

Main sources of energy losses in DC railway traction power substation are:

1. Energy losses occurring on the feeder cables of the substation and track sectioning cabins and on the return cables depend on:

- length of feeder/return cables,
- cross-section of conductors/cables,
- material of which conductors or cables are made.

2. Energy losses on the internal resistance of the substation depend on the external characteristics of the substation and the ratings of the set:

- short-circuit power on the AC busbars of the substation,
- off-load voltage of the rectifier,
- number of active rectifier sets,
- rated power of the transformer,
- short-circuit voltage of the transformer, expressed as a percentage,
- rated voltage of the set,
- rated current of the set,
- voltage drop on a single diode of the set,
- number of diodes in a branch in the case of a series connection.

Typical specification for 15kV three core armoured cables and for 15kV substation Transformers are shown in Figure 5-10 and Figure 5-11.

Nominal cross-sectional area	mm²	3x70	3x95	3x120	3x150	3x185	3x240	3x300	3x400
Diameter over conductor	mm	9.8	11.5	12.8	14.3	15.9	18.4	20.5	23.2
Approximate diameter over insulation	mm	20	21.7	23	24.5	26.1	28.6	31.1	34.2
Approximate overall diameter	mm	66	70	74	77	82	88	94	101
Approximate weight of cable	kg/m	7500	8750	9900	11100	13450	15850	18550	21900
Minimum bending radius (static)	mm	800	850	900	950	1000	1100	1150	1250
Maximum pulling tension on cable	kg	1050	1425	1800	2250	2775	3600	4500	5000
Maximum DC resistance @20°C	Ω/km	0.2680	0.1930	0.1530	0.1240	0.0991	0.0754	0.0601	0.0470
Maximum AC resistance@ 90°C	Ω/km	0.3420	0.2470	0.1960	0.1590	0.1270	0.0976	0.0786	0.0625
Inductance	mH/km	0.371	0.353	0.338	0.327	0.319	0.306	0.294	0.285
Reactance@50Hz	Ω/km	0.117	0.111	0.106	0.103	0.100	0.096	0.092	0.089
Impedance @ 50Hz @ 90°C	Ω/km	0.361	0.27	0.233	0.19	0.163	0.137	0.122	0.11
Maximum Capacitance (C)	µF/km	0.232	0.259	0.282	0.303	0.323	0.359	0.401	0.442
Maximum charging current	A/km	0.63	0.71	0.77	0.83	0.88	0.98	1.09	1.2
Short circuit ratings									
1 second short circuit-rating of conductor (90 to 250°C)	kA	9.7	13.5	17.1	21	26.3	34.6	43.4	55.6
1 second short circuit-rating of metallic screen (80 to 200°C)	kA	9.7	13.5	15.7	16.6	22.1	23.6	25.7	27.6
Continuous current carrying capacity (as per conditions detailed below)									
Direct buried	Amps	255	300	340	380	430	490	540	590
Single way ducts	Amps	215	255	290	330	370	425	470	520
In air	Amps	270	330	375	430	490	570	650	700

Figure 5-10 Typical specification for 15kV three core armoured Cables

Typical Performance Data **High Voltage –15 kV Class, Low Voltage–600V Class**

kVA	No Load Losses (Watts)	Full Load Losses (Watts)	Total Losses (Watts)	Efficiency						Maximum Efficiency
				140%	125%	100%	75%	50%	25%	
225	760	3,400	4,160	97.70	97.89	98.18	98.44	98.59	98.30	98.69@47.23%
300	900	4,635	5,535	97.68	97.87	98.19	98.47	98.65	98.44	98.66@44.07%
500	1,330	5,540	6,870	98.29	98.43	98.61	98.83	98.93	98.68	98.93@49.00%
750	1,735	9,875	11,610	98.03	98.20	98.48	98.72	98.89	98.76	98.91@41.92%
1,000	2,000	12,025	14,025	98.21	98.36	98.62	98.84	99.01	98.91	99.03@40.78%
1,500	2,900	15,720	18,620	98.42	98.66	98.77	98.97	99.10	98.98	99.11@42.95%
2,000	3,535	21,750	25,285	98.38	98.62	98.75	98.96	99.11	99.03	99.13@40.31%
2,500	4,400	23,750	28,150	98.67	98.69	98.89	99.06	99.18	99.07	99.19@43.04%
3,000	5,385	28,450	33,835	98.67	98.69	98.88	99.06	99.17	99.05	99.18@43.61%
3,750	7,700	34,850	42,550	98.67	98.69	98.88	99.04	99.13	98.96	99.13@47.00%
5,000*	9,650	46,750	56,400	98.67	98.69	98.88	99.05	99.15	99.00	99.16@45.43%
7,500*	11,950	56,500	68,450	98.85	98.94	99.10	99.23	99.31	99.18	99.31@45.99%
10,000*	16,515	66,923	83,440	98.96	99.04	99.17	99.28	99.34	99.18	99.34@49.68%

*5,000; 7,500; 10,000 kVA are listed with 5 kV secondaries.

Typical Performance Data

kVA	%IZ	%IR	%IX	X/R Ratio	Regulation			
					1.0 PF	.9 PF	.8 PF	.7 PF
225	4.00	1.52	3.72	2.46	1.58	3.01	3.45	3.71
300	4.00	1.55	3.69	2.39	1.61	3.03	3.47	3.73
500	4.50	1.11	4.37	3.94	1.20	2.96	3.54	3.92
750	5.75	1.32	5.60	4.05	1.41	3.12	3.67	4.02
1,000	5.75	1.20	5.63	4.68	1.36	3.64	4.41	4.90
1,500	5.75	1.05	5.65	5.39	1.21	3.51	4.31	4.82
2,000	5.75	1.09	5.64	5.19	1.25	3.55	4.33	4.84
2,500	5.75	0.95	5.67	5.97	1.11	3.44	4.24	4.77
3,000	5.75	0.95	5.67	5.98	1.11	3.44	4.24	4.77
3,750	5.75	0.93	5.68	6.11	1.09	3.42	4.23	4.76
5,000	5.75	0.94	5.68	6.08	1.10	3.42	4.23	4.76
7,500	5.50	0.75	5.45	7.23	0.90	3.16	3.95	4.47
10,000	5.50	0.67	5.47	8.17	0.82	3.09	3.89	4.42

Figure 5-11 Typical specifications for 15kV substation Transformers

5.4 Station losses

Railway stations are considered as industrial facilities in relation to the provided power. It is known that the power, which is necessary to run a station, is taken from the catenary due to economic factors. Due to the lack of information and the existing difficulties to obtain actual data of a station, this calculation has been based on governmental documents[14], which provide power data per area for industrial activities. Regarding that, a standard subway station area is above 1000 m^2, the estimated power is 50 W/m^2.

Table 5-7 Estimated power in industrial facilities

Surface of the area [m^2]	Minimum power expected [kW]
$S \leq 300$	15
$300 < S \leq 1000$	15 + 0.05·(S-300)
$1000 < S$	0.05·S

[14] Boletín oficial de la Junta de Andalucía 14 de octubre de 2004, de la Dirección General de Industria, Energía y Minas, sobre previsión de cargas eléctricas y coeficientes de simultaneidad en áreas de uso residencial y áreas de uso industrial

6 Case studies with simulations

6.1 Numerical simulations of Metro de Madrid – Line 2

6.1.1 Data interpretation

Line 2 of MDM is 14.031 km with 20 stations and 5 traction substations. As indicated in the appendix, the trains stop at every station. The total journey time between the two termini is around 27min. The operating voltage of this line is 1,500 V DC.

6.1.2 Train motion simulation

Using the data of the previous section and considering the speed limit on the line, the speed and power diagram of each individual train is given by Figure 6-1and Figure 6-2, valid respectively for trains travelling from Cuatro Caminos to Las Rosas and vice versa. The train acceleration shows the typical constant effort and constant power regions typical of traction systems. The amount of coasting has been selected to keep the deceleration rate within the limit and guarantee that the train reaches the next station on time. In the model, there are no train delays or other causes disrupting the train service. Additionally, it has been assumed an identical dwelling time for all the stations and all the trains. The time step of the simulation has been set to 1 s. The simulations are carried out when full service is running, i.e. excludes operations in the first hour and the last hour of the service when the number of trains is reduced.

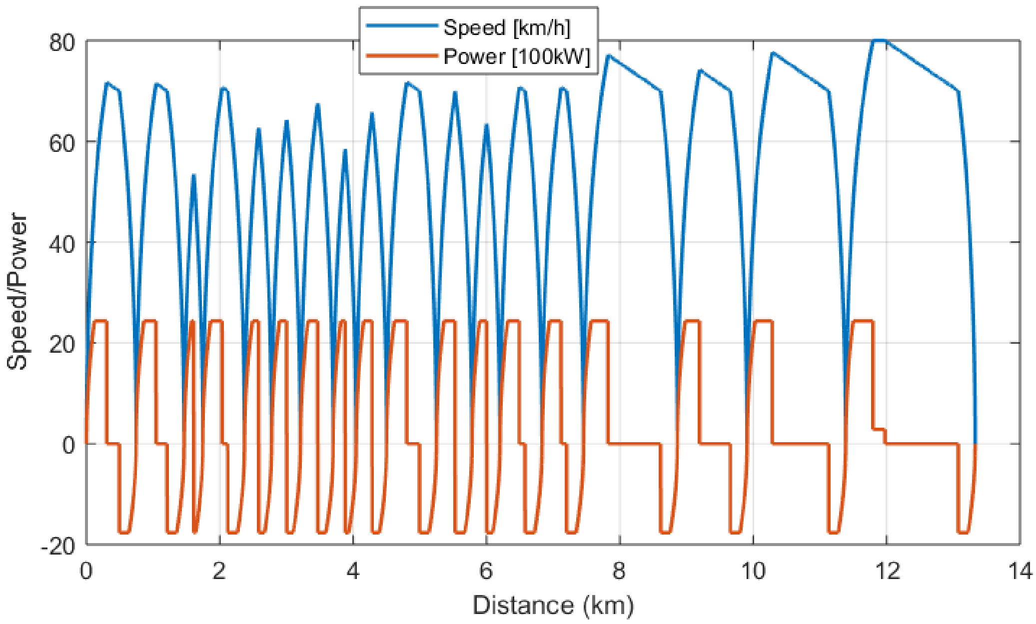

Figure 6-1 Speed and profiles of a train travelling from Cuatro Caminos to Las Rosas (up)

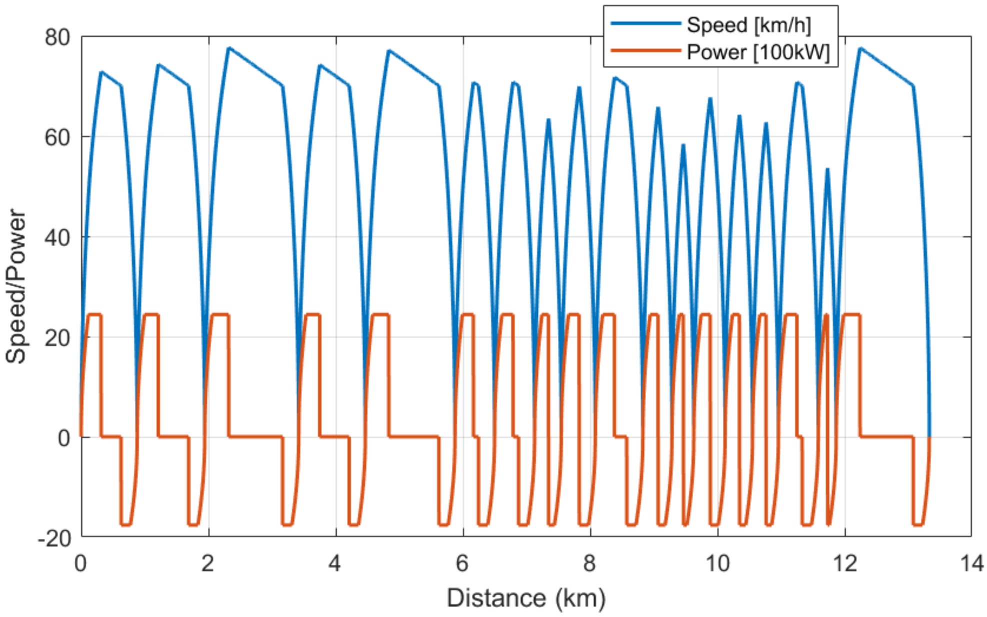

Figure 6-2. Speed and power profiles of a train travelling from Las Rosas to Cuatro Caminos (down)

6.1.3 Power network simulation

6.1.3.1 Energy consumption (full-time simulation)

The system energy consumptions within the headway period are shown in Table 6-1 various headway values. This refers to the energy drawn from all the TPSS during train service. The table has the following rows:
E_s = Energy supplied by all the substations to the traction system within the headway time
$P_{s,mean}$ = Average power supplied by all the substations within the headway time
$E_{s,loss}$ = Energy losses of all the substations
$E_{t,loss}$ = Energy losses of the electrification system (overhead supply and return rails)
$P_{loss,mean}$ = Average power losses (substation and electrification) within the headway time
$E_{traction,demand}$ = Energy required by all the train to accelerate and coast
$E_{traction}$ = Energy actually drawn by all the train to complete the journey
$E_{braking,available}$ = Energy available from all the train for regenerative braking
$E_{braking}$ = Energy actually regenerated by trains
η_{regen} = Efficiency of regenerative braking, calculated as $E_{braking}$ / $E_{braking,available}$

Table 6-1 Energy consumption with various headways

Headway	[s]	120	180	240	300	360	420	480	540	600	660
E_s	[kWh]	257	263	300	259	300	286	317	326	309	292
$P_{s,mean}$	[MW]	7.71	5.30	4.5	3.11	3.00	2.45	2.38	2.17	1.85	1.59
$E_{s,loss}$	[kWh]	7.7	7.9	9.0	7.8	9.0	8.6	9.5	9.8	9.3	8.8
$E_{t,loss}$	[kWh]	11.0	4.8	8.5	6.3	6.7	6.7	7.0	6.4	7.4	5.9
$P_{loss,mean}$	[MW]	0.56	0.25	0.26	0.17	0.16	0.13	0.12	0.11	0.10	0.08
$E_{traction,demand}$	[kWh]	450	450	450	450	450	450	450	450	450	450
$E_{traction}$	[kWh]	450	450	450	450	450	450	450	450	450	450
$E_{braking,available}$	[kWh]	273	273	273	273	273	273	273	273	273	273

$E_{braking}$	[kWh]	248	236	204	242	202	216	186	177	194	209
η_{regen}	[%]	91%	86%	75%	89%	74%	79%	68%	65%	71%	76%

The results show that the energy consumption of the traction system increases when the headway decreases, as there are more trains running simultaneously on the line. In fact, the average power increases from 1.59 MW when the headway is 660 s to 7.71 MW when the headway is 120 s. Similar trend can be identified on power losses, and their impact increases from 5% when the headway is 660 s to 7% when the headway is 120 s.

The losses variation however is different when the headway changes. In fact, the energy lost in the transmission system increases significantly for shorter headways. The split of transmission and substation losses is 40-60 when the headway is 660 s and is 59-41 when the headway is 120 s. This can be explained by the higher regeneration rate when the headway is shorter as less energy is supplied by traction power substation (TPSS) and more energy is exchanged between trains using the electrification network. In fact, the energy actually regenerated by trains increases with respect to the maximum available braking energy and the efficiency of the regenerative braking increases from 76% when the headway is 660 s to 91% when the headway is 120 s.

6.1.3.2 Instantaneous results

This section presents results of the simulation captured at a random second for a headway of 120 s. The shortest headway has been selected to analyse the case of highest average power demand from the traction network. At this second, there are 25 trains running simultaneously on the network. Figure 6-3 shows the value of the voltage of the overhead lines of the two tracks. The overhead lines are bonded at every TPSS only. The voltage of the running rails is around 0 V and it has not been reported in this figure. It can be seen that at every instant there are area of the electrification system where the voltage is lower and other where is higher, but no conditions of undervoltage or overvoltage have been identified. Therefore, it can be concluded that the traction system does not cause significant concern in terms of voltage regulation.

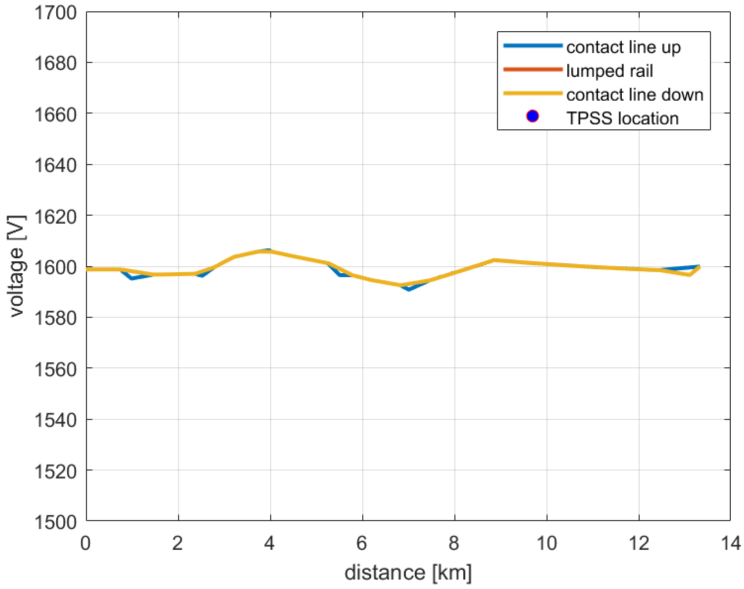

Figure 6-3 Voltage of the electrification system with a headway of 120 s

The previous figure has been overlapped with the position of the train to obtain the instantaneous train voltage as shown in Figure 6-4. The maximum and minimum voltages are 1620 V and 1580 V, i.e. + 8% and +5% of the nominal voltage. These values are within the normal operating range of the line.

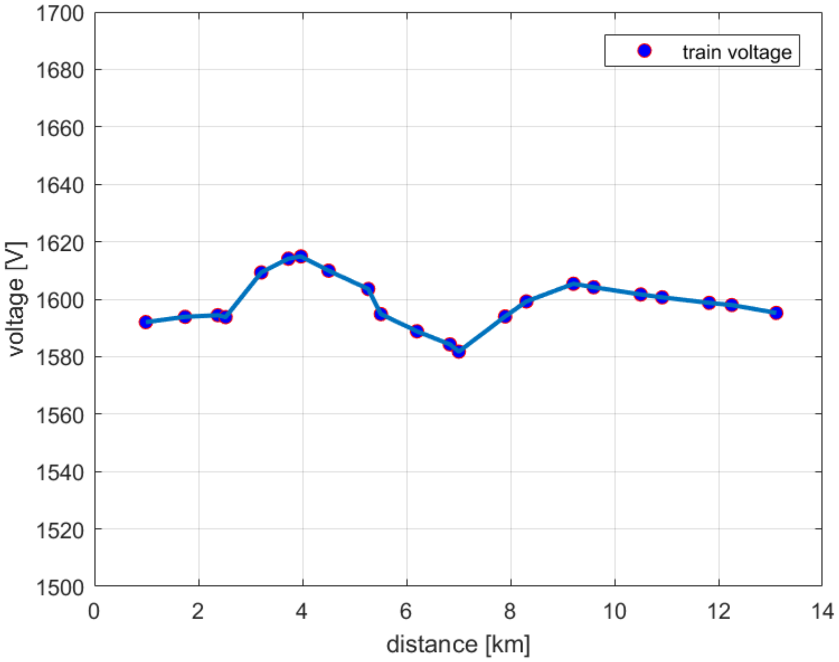

Figure 6-4. Train voltages with a headway of 120s

Table 6-2 illustrates the output voltage, current and power of the 5 TPSS on the line. The loading factor is each TPSS is between 33% and 42%. This is compatible with normal traction systems, as redundancy is necessary to run a full timetable even when one substation is completely out of service.

Table 6-2 Instantaneous quantities for the TPSS

No.	Location [m]	Voltage [V]	Current [A]	Power [kW]
1	745	1598	1516	2502
2	3209	1609	1193	1968
3	5249	1604	1353	2232
4	8865	1607	1274	2101
5	13332	1601	1441	2378

Table 6-3 shows the main quantities of all the trains travelling on the line. In this table, the direction is up for 0 and down for 1. Also, the meaning of operating mode is 0 for normal, 1 for overvoltage and 2 for undervoltage. The table confirms that all the trains are running normally, as the voltage of the line is within the limits. This is also confirmed by the fact that the trains draw an actual power equal to their power demand, i.e. the power necessary to follow the desired speed diagram.

The specific operating conditions of the trains is variable as expected from normal operations. The trains drawing a large amount of current are accelerating; the trains drawing a small amount of current are coasting or braking with dissipative braking (on-board rheostats); and the train drawing a negative power are braking with regenerative braking. The voltage level follows the current drawn by the trains. Trains accelerating show the lowest voltage levels and train decelerating show the highest voltage levels. In this situation, all the braking trains regenerate power to other trains, as none of them reaches the threshold for activating the braking rheostats.

Table 6-3 Instantaneous quantities for the trains on the line

No.	Location [m]	Direction	Operating mode	Voltage [V]	Current [A]	Power demand [kW]	Actual Power [kW]
1	989	0	0	1592	1557	2479	2479
2	1743	0	0	1594	27	43	43
3	2373	1	0	1594	25	40	40
4	2522	0	0	1594	1555	2479	2479
5	3208	1	0	1609	218	350	350
6	3208	0	0	1609	27	44	44
7	3730	1	0	1614	-519	-837	-837
8	3972	0	0	1615	-863	-1394	-1394
9	4502	0	0	1610	28	46	46
10	4504	1	0	1610	28	44	44
11	5265	1	0	1604	-374	-599	-599
12	5508	0	0	1595	1554	2479	2479
13	6201	0	0	1589	28	44	44
14	6202	1	0	1589	213	339	339
15	6835	1	0	1584	-50	-79	-79
16	7007	0	0	1582	1567	2479	2479
17	7898	1	0	1594	25	40	40
18	8307	0	0	1599	25	40	40
19	9211	1	0	1605	25	40	40
20	9599	0	0	1604	25	40	40
21	10505	1	0	1602	25	40	40
22	10917	0	0	1601	25	40	40
23	11820	1	0	1599	25	40	40
24	12255	0	0	1598	25	40	40
25	13110	1	0	1595	1554	2479	2479

6.1.4 Power analysis of traction power substation (TPSS)

This section investigates in more details the power of the TPSS and the impact on the presence of an additional converter enabling energy regeneration to the distribution grid. The analysis has been repeated for different headways, as they affect the average power consumption and losses on the electrification system and the substations.

6.1.4.1 Headway of 120 s

Figure 6-5 shows the power of each substation during a time interval equal to the headway (120 s), this is because these diagrams are periodic of the headway time at steady-state. The instantaneous power of the TPSS is significantly variable due to the different operating conditions of the trains and the different position on the line. Additionally, the power of all TPSS is always positive as diodes do not allow any regenerative braking back to the 15 kV power distribution grid.

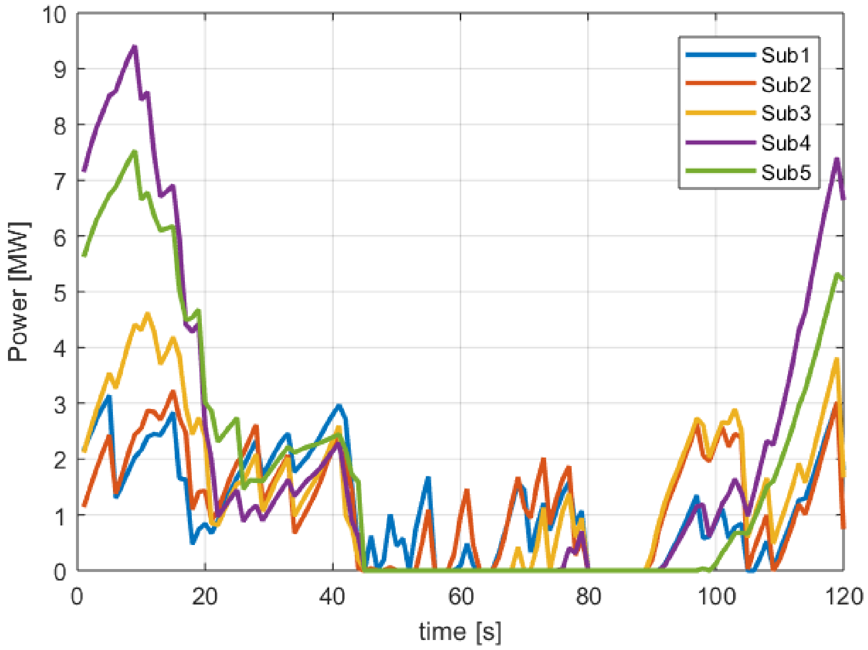

Figure 6-5. Power of each traction substation

In order to compare better the actual loading of TPSS, Table 6-4 shows the maximum, minimum and average power of each substation. All the substations have some instants where do not supply any power to the trains. This is normal for DC traction system, as trains are powered mainly by the two adjacent substations. Therefore, this situation occurs more often for the TPSS closer to the two ends of the line.

Table 6-4 Maximum, minimum and average power of each TPSS

No.	Maximum power [MW]	Minimum power [MW]	Average power [MW]
1	3.14	0	1.13
2	3.23	0	1.22
3	4.62	0	1.41
4	9.41	0	2.12
5	7.54	0	1.83

The table also shows that the maximum power is several times higher the average power, with factors between 278% and 444%.

The instantaneous power of some TPSS even exceeds the rated power, even if only for few tens of seconds. This is again acceptable, as all TPSS can be overloaded for a short period of time. The heaviest overload is 156% for substation 4, which can be considered of mild level. For comparison, in the UK typical duty classes of TPSS are class F (120% overloading for 60 minutes, 150% for 5 minutes and 300% for 1 minute) class G (177.5% for 60 minutes, 283% for 5 minutes and 382.9% for 1 minute) and class H (100% for 60 minutes, 150% for 1 minute).

The energy consumption has been recalculated when one of the TPSS is reversible for the presence of the sSOP, as shown in Table 6-5. The number 0 means that no TPSS are reversible (baseline case), whereas 1 means that TPSS 1 is reversible and so on. Table 6-5 shows that when the sSOP is located at TPSS 5 the line achieves the lowest energy consumption. With the introduction of one sSOP, the efficiency of regeneration is improved for all the configurations.

Table 6-5 Energy consumption with a sSOP installed at one of the TPSS

Location of the sSOP		0	1	2	3	4	5
Headway	[s]	120	120	120	120	120	120
E_s	[kWh]	257	251	251	250	237	**235**
$E_{s,rectified}$	[kWh]	257	257	257	258	264	262
$E_{s,inverted}$	[kWh]	0.0	-5.9	-6.3	-8.1	-27.2	-26.7
$E_{s,loss}$	[kWh]	7.7	8.0	8.0	8.2	9.4	9.3
$E_{t,loss}$	[kWh]	11.0	11.3	11.3	11.5	10.7	10.7
$E_{traction,demand}$	[kWh]	450	450	450	450	450	450
$E_{traction}$	[kWh]	450	450	450	450	450	450
$E_{braking,available}$	[kWh]	273	273	273	273	273	273
$E_{braking}$	[kWh]	248	254	255	257	270	271
η_{regen}	[%]	91%	93%	93%	94%	99%	99%

Figure 6-6 to Figure 6-10 describe how the power curves of TPSS are affected for the presence of one sSOP at one of the TPSS. The regenerative power of the sSOP depends on the control scheme of the power converter. In this simulation, there is a fixed linear voltage regulation characteristic for the converter. The analysis of the various configuration shows that the maximum regenerative power of the sSOP is around 5 MW, when the sSOP is installed at TPSS 5.

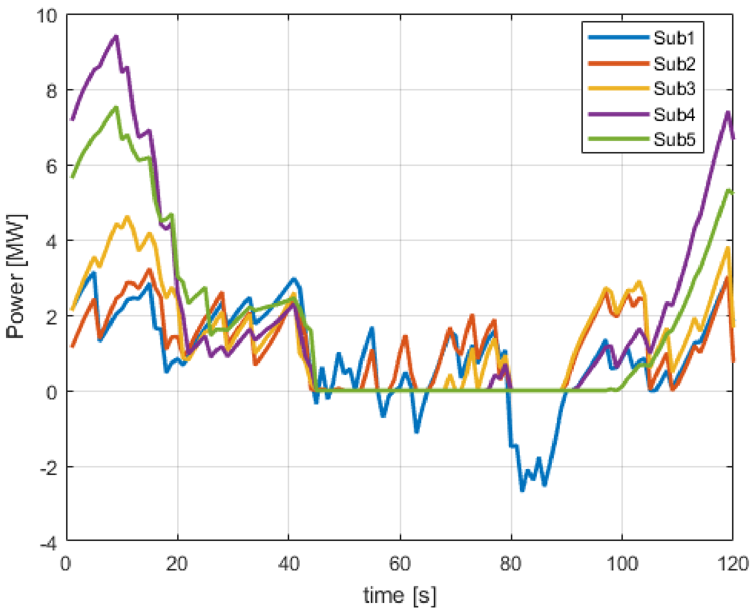

Figure 6-6. Instantaneous power of TPSS when sSOP is at TPSS 1

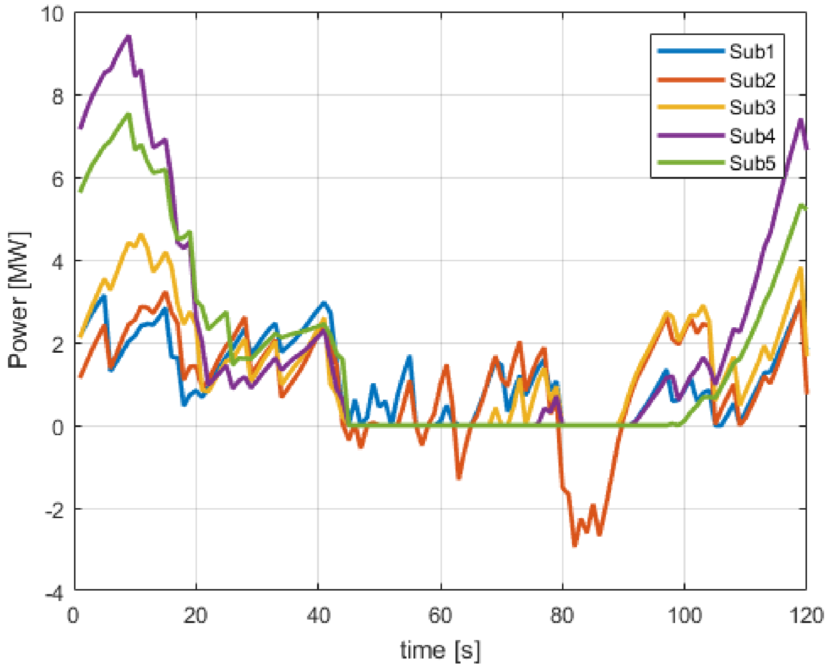

Figure 6-7. Instantaneous power of TPSS when sSOP is at TPSS 2

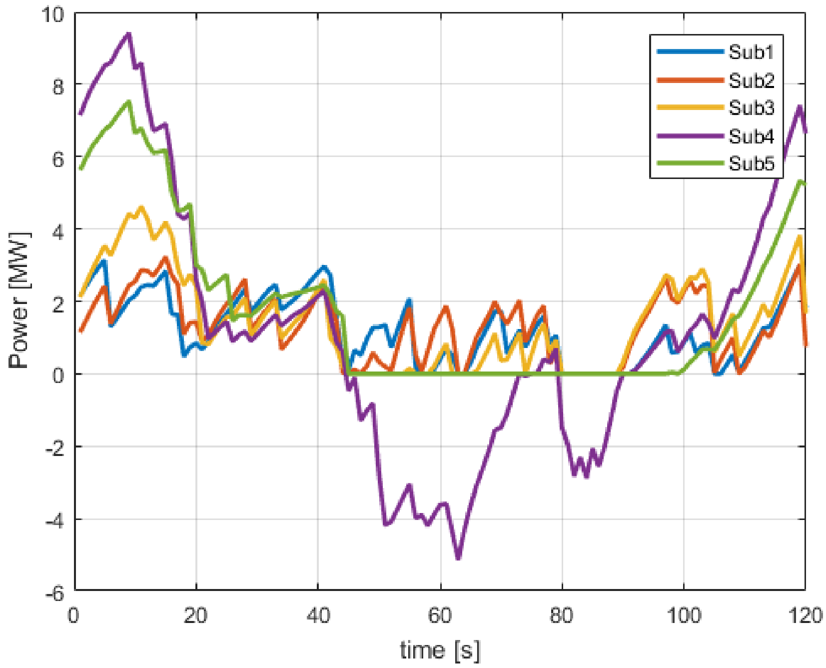

Figure 6-8. Instantaneous power of TPSS when sSOP is at TPSS 3

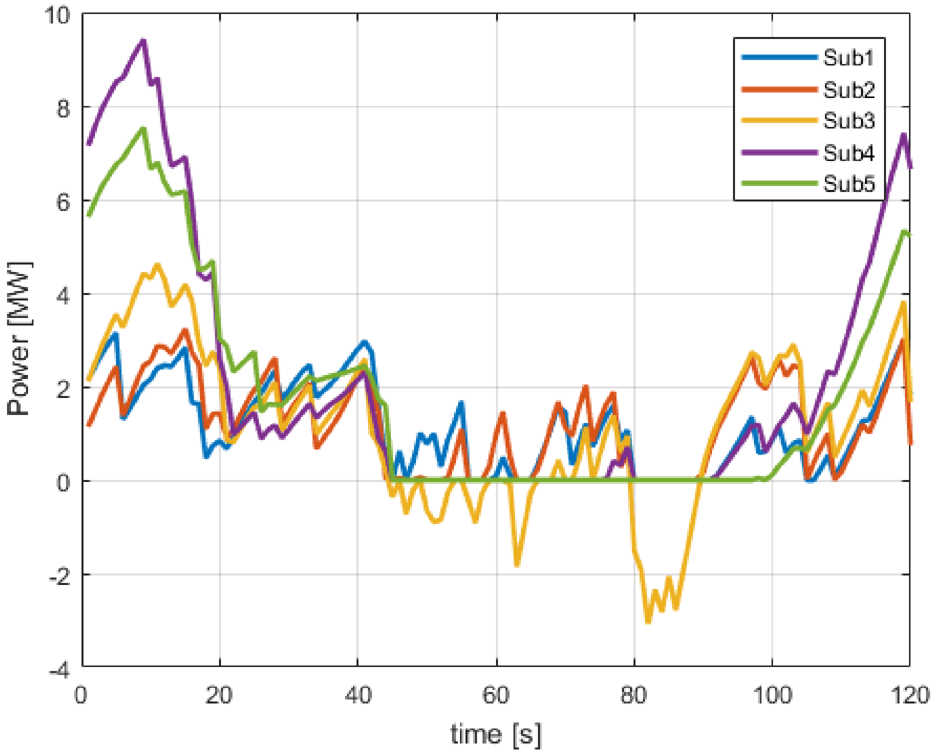

Figure 6-9. Instantaneous power of TPSS when sSOP is at TPSS 4

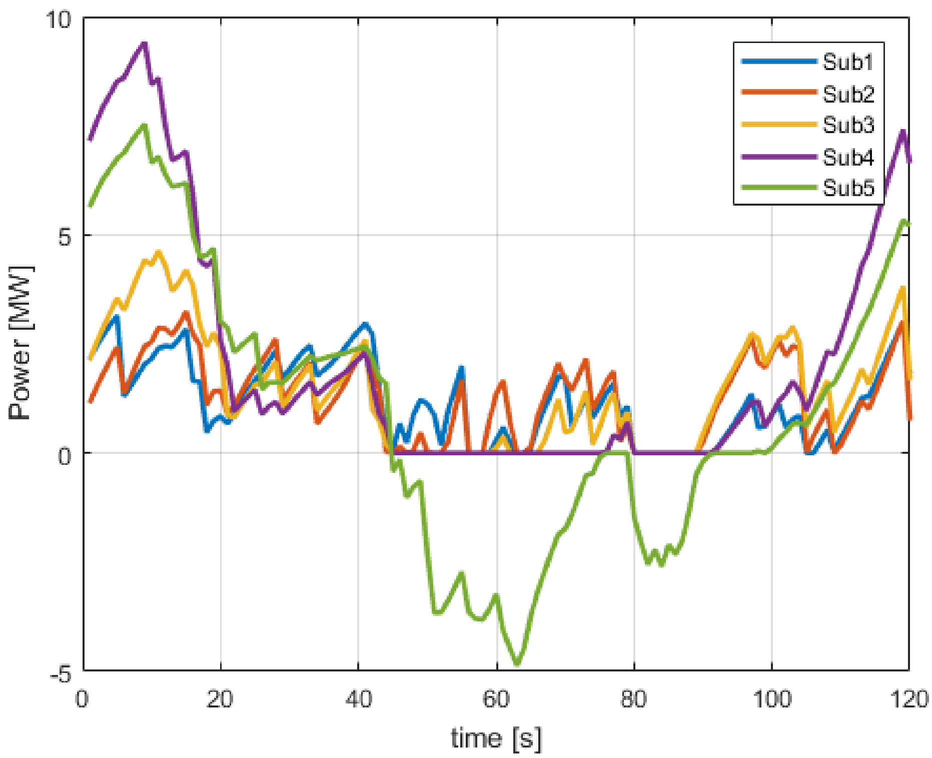

Figure 6-10. Instantaneous power of TPSS when sSOP is at TPSS 5

6.1.4.2 Headway=360s

The simulations have been repeated for a headway of 360 s and the results are shown in Figure 6-11.

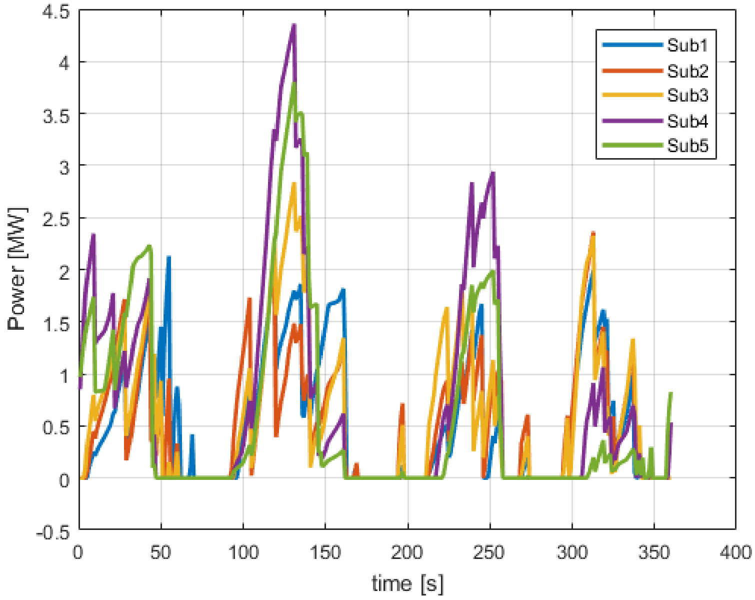

Figure 6-11. Power of each traction substation

It is evident the significant impact not only in terms of instantaneous power, but also in term of maximum, minimum and average power, as shown below. The diagram of power consumption is much more variable and the ratio between maximum power and average power varies from 402% to 597%. Additionally, there are no TPSS overloaded in this scenario.

Table 6-6 Maximum, minimum and average power of each substation

No.	Maximum power [MW]	Minimum power [MW]	Average power [MW]
1	2.13	0	0.53
2	2.36	0	0.53
3	2.84	0	0.61
4	4.36	0	0.73
5	3.80	0	0.60

Table 6-7 shows the impact on the energy consumption.

Table 6-7 Energy consumption with various headways in [kWh]

Location of the sSOP		0	1	2	3	4	5
Headway	[s]	360	360	360	360	360	360
E_s	[kWh]	300	248	245	241	**239**	249
$E_{s,rectified}$	[kWh]	300	301	301	301	304	305
$E_{s,inverted}$	[kWh]	0.0	-53.0	-55.9	-60.0	-64.9	-55.9
$E_{s,loss}$	[kWh]	9.0	11.8	12.0	12.2	12.5	12.1
$E_{t,loss}$	[kWh]	6.7	8.6	8.8	8.8	8.1	8.3
$E_{traction,demand}$	[kWh]	450	450	450	450	450	450

$E_{traction}$	[kWh]	450	450	450	450	450	450
$E_{braking,available}$	[kWh]	273	273	273	273	273	273
$E_{braking}$	[kWh]	202	259	262	266	268	258
η_{regen}	[%]	74%	95%	96%	97%	98%	95%

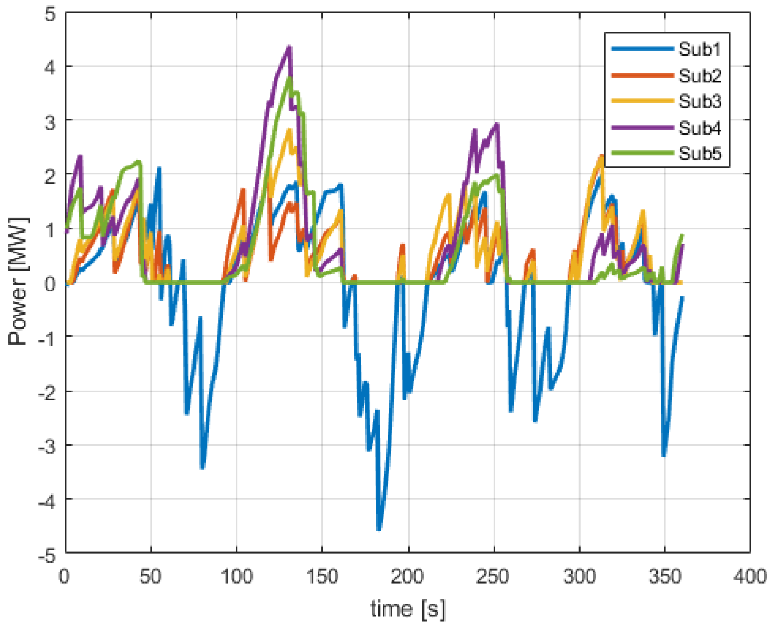

Figure 6-12 Instantaneous power of TPSS when sSOP is at TPSS 1

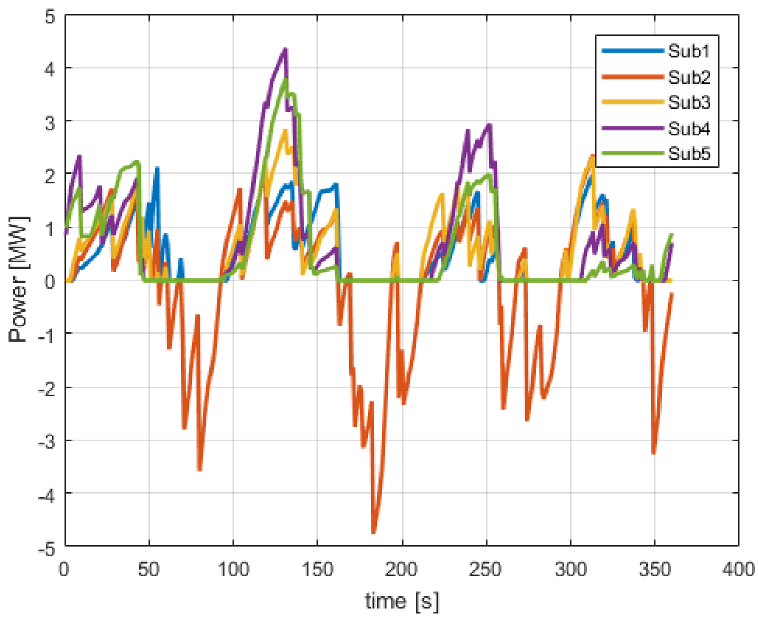

Figure 6-13 Instantaneous power of TPSS when sSOP is at TPSS 2

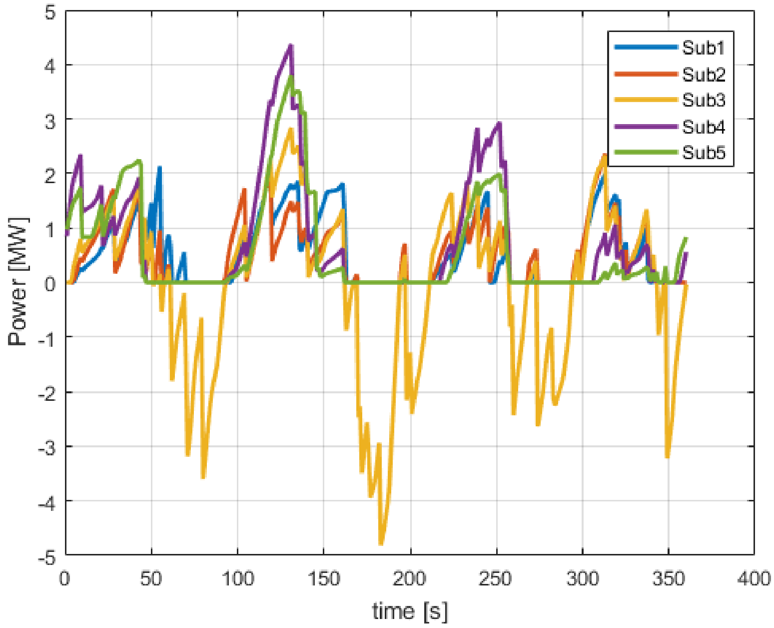

Figure 6-14 Instantaneous power of TPSS when sSOP is at TPSS 3

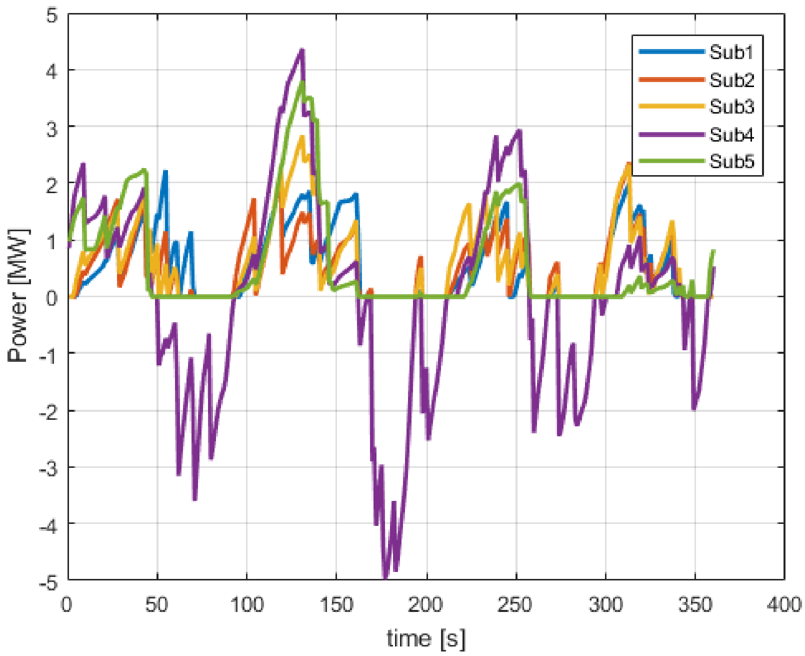

Figure 6-15 Instantaneous power of TPSS when sSOP is at TPSS 4

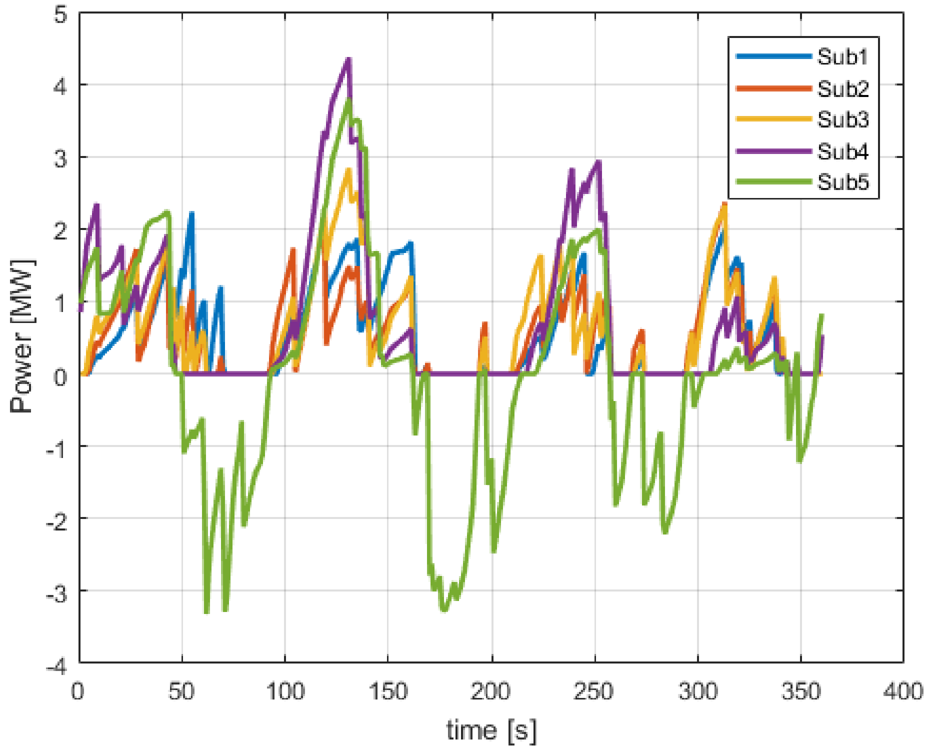

Figure 6-16 Instantaneous power of TPSS when sSOP is at TPSS 5

6.1.4.3 Headway=600s

The simulations have been repeated for a headway of 600 s. The results are shown in following figures and tables.

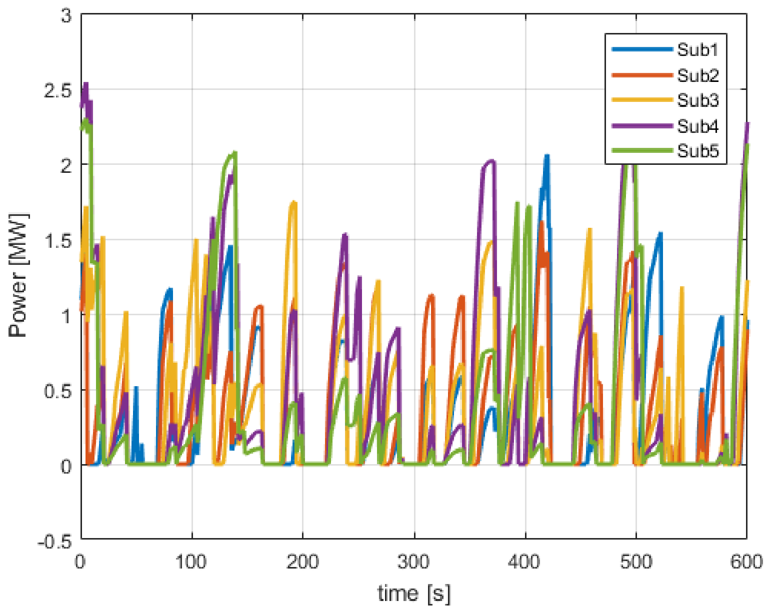

Figure 6-17 Power of each substation

Table 6-8 Maximum, minimum and average power of each substation

No.	Maximum power [MW]	Maximum power [MW]	Average power [MW]
1	2.06	0	0.31
2	1.62	0	0.34
3	1.74	0	0.37
4	2.54	0	0.46
5	2.30	0	0.36

Table 6-9 Energy consumption with various headways in [kWh]

Inverter information	0	1	2	3	4	5
Headway [s]	600	600	600	600	600	600
E_sub_act	309	252	244	240	236	244
E_sub_rectified	309	310	310	310	311	312
E_sub_inverted	0.0	-58.0	-65.6	-70.0	-74.5	-67.3
E_sub_loss_act_all	9.3	12.4	12.8	13.0	13.3	12.9
E_trans_loss_all	7.4	10.2	9.9	9.6	9.1	9.6
E_traction_demand_all	450	450	450	450	450	450
E_traction_all	450	450	450	450	450	450
E_brake_all	273	273	273	273	273	273
E_regen_all	194	257	265	269	273	265
Regen efficiency (E_regen_all/ E_brake_all)	71%	94%	97%	99%	100%	97%
E_auxiliary	36	36	36	36	36	36

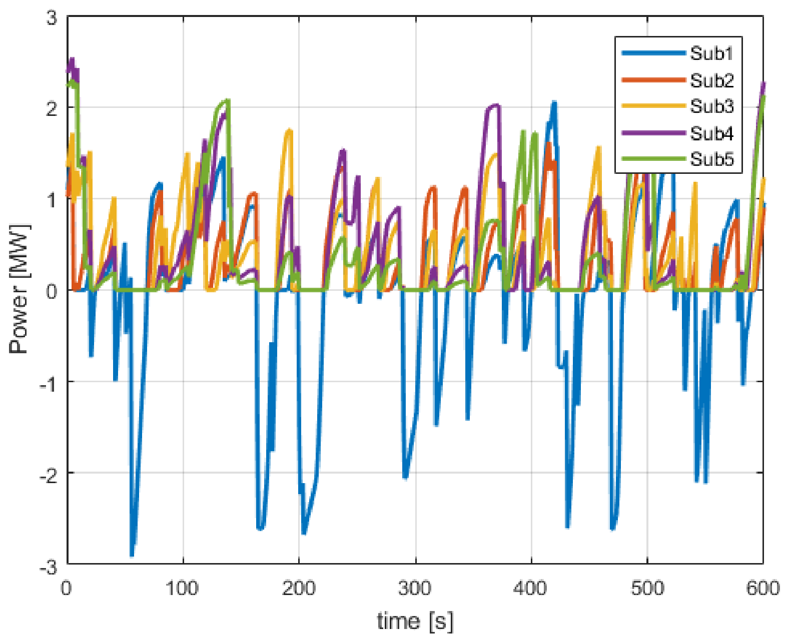

Figure 6-18 Instantaneous power of TPSS when sSOP is at TPSS 1

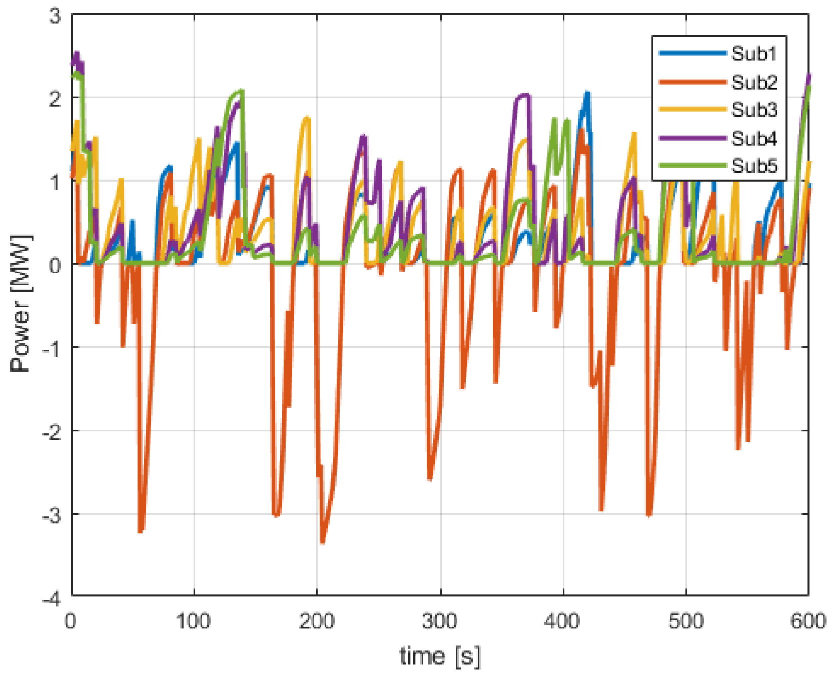

Figure 6-19 Instantaneous power of TPSS when sSOP is at TPSS 2

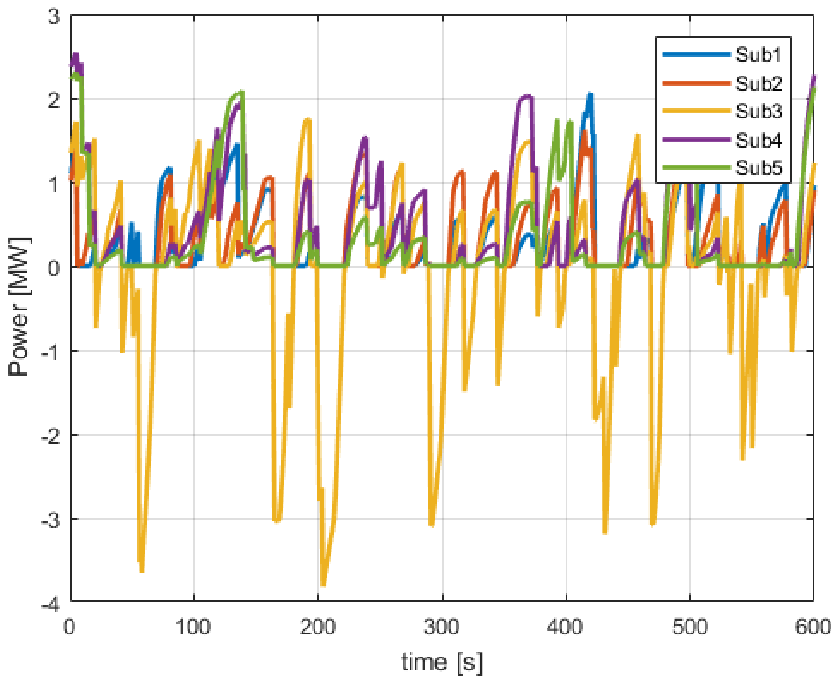

Figure 6-20 Instantaneous power of TPSS when sSOP is at TPSS 3

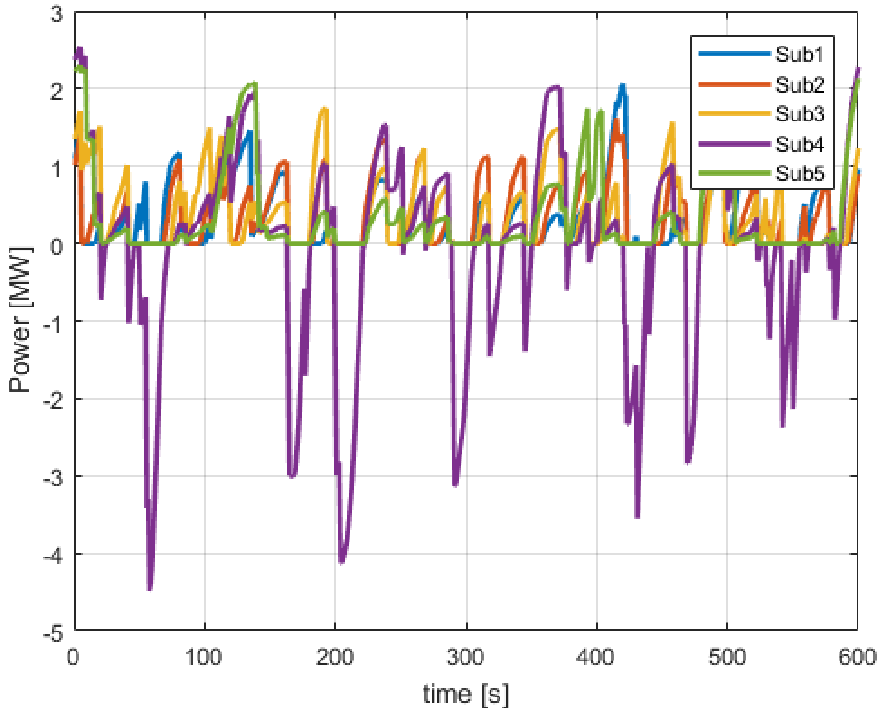

Figure 6-21 Instantaneous power of TPSS when sSOP is at TPSS 4

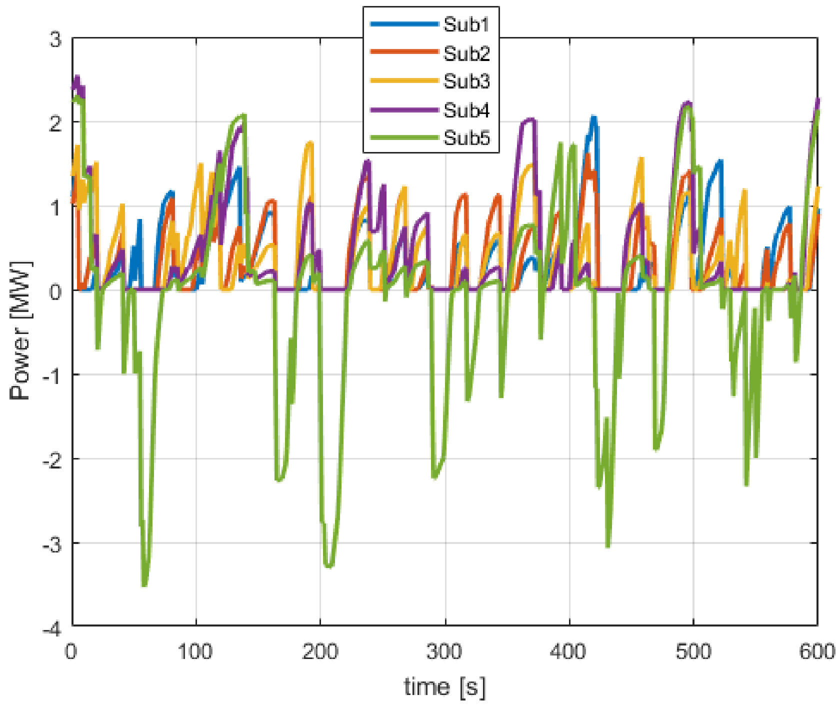

Figure 6-22 Instantaneous power of TPSS when sSOP is at TPSS 5

6.2 Numerical simulations of Metro de Madrid – Line 12

6.2.1 Data interpretation

Line 12 of MDM is a 40.9 km circle line with 28 stations and 11 traction substations. The trains depart from Puerta del Sur, and stop at every station, and finally return Puerta del Sur. The total journey time is around 60 min. The operating voltage of this line is 1,500 V DC.

6.2.2 Train motion simulation

Using the data of the previous section and considering the speed limit on the line, the speed and power diagram of each individual train is given by Figure 6-23 and Figure 6-24, valid respectively for trains travelling from Puerta del Sur to Parque Lisboa and vice versa. The trains acceleration shows the typical constant effort and constant power regions typical of traction systems. The amount of cruising has been selected to keep the speed within the limit and guarantee that the train reaches the next station on time. In the model, there are no train delays or other causes disrupting the train service. Additionally, it has been assumed an identical dwelling time for all the stations and all the trains. The time step of the simulation has been set to 1 s. The simulations are carried out when full service is running, i.e. excludes operations in the first hour and the last hour of the service when the number of trains is reduced.

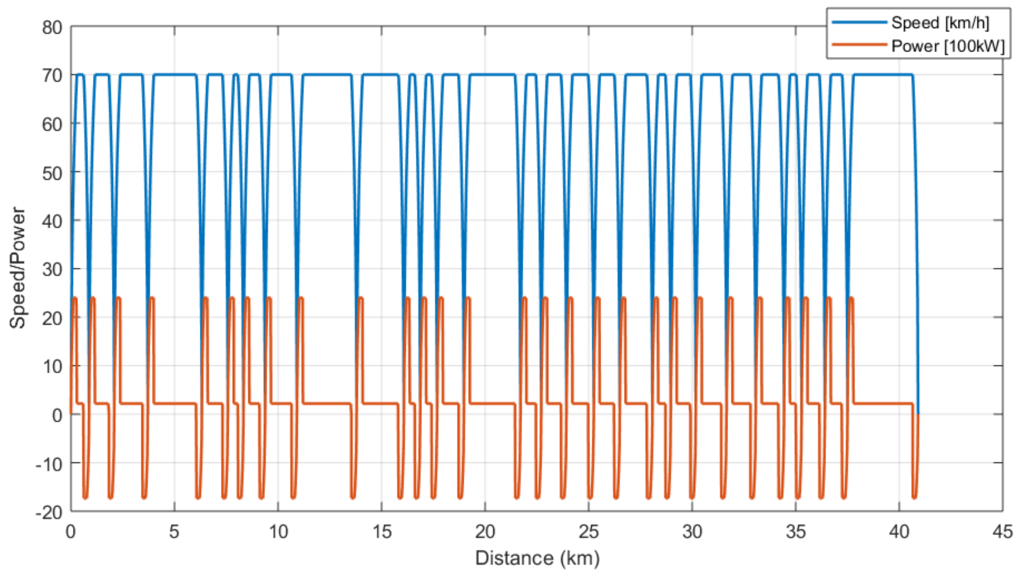

Figure 6-23. Speed and profiles of a train travelling from Puerta del Sur to Parque Lisboa (up)

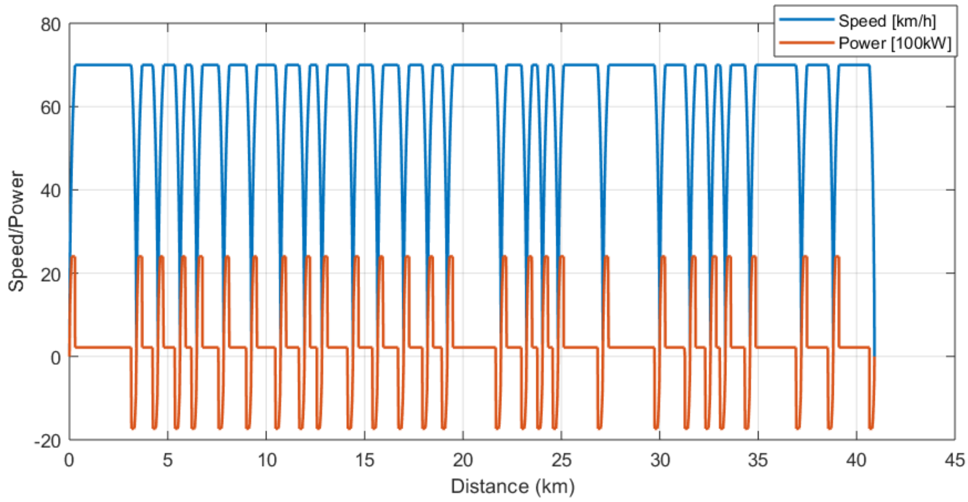

Figure 6-24. Speed and power profiles of a train travelling from Puerta del Sur to San Nicasio (down)

6.2.3 Power network simulation

6.2.3.1 Energy consumption (full-time simulation)

The system energy consumptions within the headway period are shown in Table 6-10 for various headway values. This refers to the energy drawn from all the TPSS during train service. The table has the following rows:

E_s = Energy supplied by all the substations to the traction system within the headway time
$P_{s,mean}$ = Average power supplied by all the substations within the headway time
$E_{s,loss}$ = Energy losses of all the substations
$E_{t,loss}$ = Energy losses of the electrification system (overhead supply and return rails)
$P_{loss,mean}$ = Average power losses (substation and electrification) within the headway time
$E_{traction,demand}$ = Energy required by all the train to accelerate and coast
$E_{traction}$ = Energy actually drawn by all the train to complete the journey
$E_{braking,available}$ = Energy available from all the train for regenerative braking
$E_{braking}$ = Energy actually regenerated by trains
η_{regen} = Efficiency of regenerative braking, calculated as $E_{braking} / E_{braking,available}$

Table 6-10 Energy consumption with various headways

Headway	[s]	120	180	240	300	360	420	480	540	600	660
E_s	[kWh]	618	616	616	636	617	643	621	622	656	675
$P_{s,mean}$	[MW]	5.15	3.42	2.57	2.12	1.71	1.53	1.29	1.15	1.09	1.02
$E_{s,loss}$	[kWh]	18.5	18.5	18.5	19.1	18.5	19.3	18.6	18.7	19.7	20.3
$E_{t,loss}$	[kWh]	12.5	10.7	10.6	12.4	11.7	12.7	12.5	14.4	11.9	13.9
$P_{loss,mean}$	[MW]	0.26	0.16	0.12	0.10	0.08	0.08	0.06	0.06	0.05	0.05
$E_{traction,demand}$	[kWh]	861	861	861	861	861	861	861	861	861	861
$E_{traction}$	[kWh]	861	861	861	861	861	861	861	861	861	861
$E_{braking,available}$	[kWh]	453	453	453	453	453	453	453	453	453	453
$E_{braking}$	[kWh]	453	453	453	435	453	428	450	451	415	399
η_{regen}	[%]	100%	100%	100%	96%	100%	95%	99%	100%	92%	88%

The results show that the energy consumption of the traction system increases when the headway decreases, as there are more trains running simultaneously on the line. In fact, the average power increases from 1.02 MW when the headway is 660 s to 5.16 MW when the headway is 120 s. Similar trend can be identified on power losses, but the ratio of the power losses to the respective power consumption is around 5% with various headways.

The energy losses vary with the headway changes, but not significantly. When the substation energy supply is high, for example when headway is 660 s, the energy loss is higher. The substation loss is determined by the power from substation, and the transmission loss depends on the power flowing in the network. The efficiency of regenerative braking decreases with the headway. In this case study, the efficiency of regeneration braking is high for this route, which is between 88% and 100%. One reason for the high efficiency is that the DC network is a long circle line, which allows the regenerative power to flow both sides. It is not suitable to use SOP for this line, as the available regenerative braking energy for conversion is low.

6.2.3.2 Instantaneous results

This section presents results of the simulation captured at a random second for a headway of 120 s. The shortest headway has been selected to analyse the case of highest average power demand from the traction network. At this second, there are 60 trains running simultaneously on the network. Fig. 3 shows the value of the voltage of the overhead lines of the two tracks. The overhead lines are bonded at every TPSS only. The voltage of the running rails is around 0 V and it has not been reported in this figure. It can be seen that at every instant there are area of the electrification system where the voltage is lower and other where is higher, but no conditions of undervoltage or overvoltage have been identified. Therefore, it can be concluded that the traction system does not cause significant concern in terms of voltage regulation.

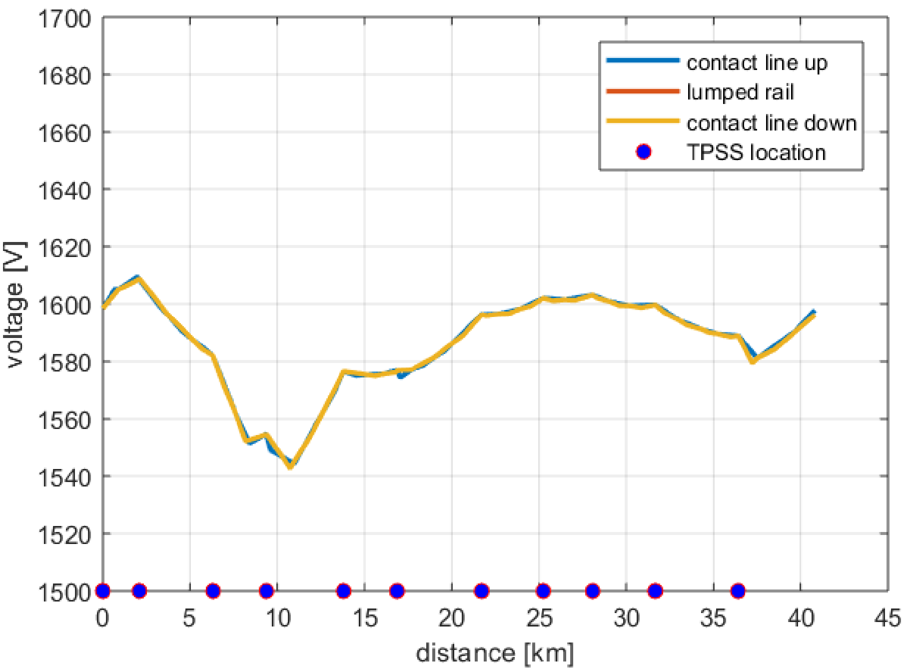

Figure 6-25 Voltage of the electrification system with a headway of 120 s

The previous figure has been overlapped with the position of the train to obtain the instantaneous train voltage as shown in Figure 6-26 The maximum and minimum voltages are 1638 V and 1490 V, i.e. + 9% and -1% of the nominal voltage. These values are within the normal operating range of the line.

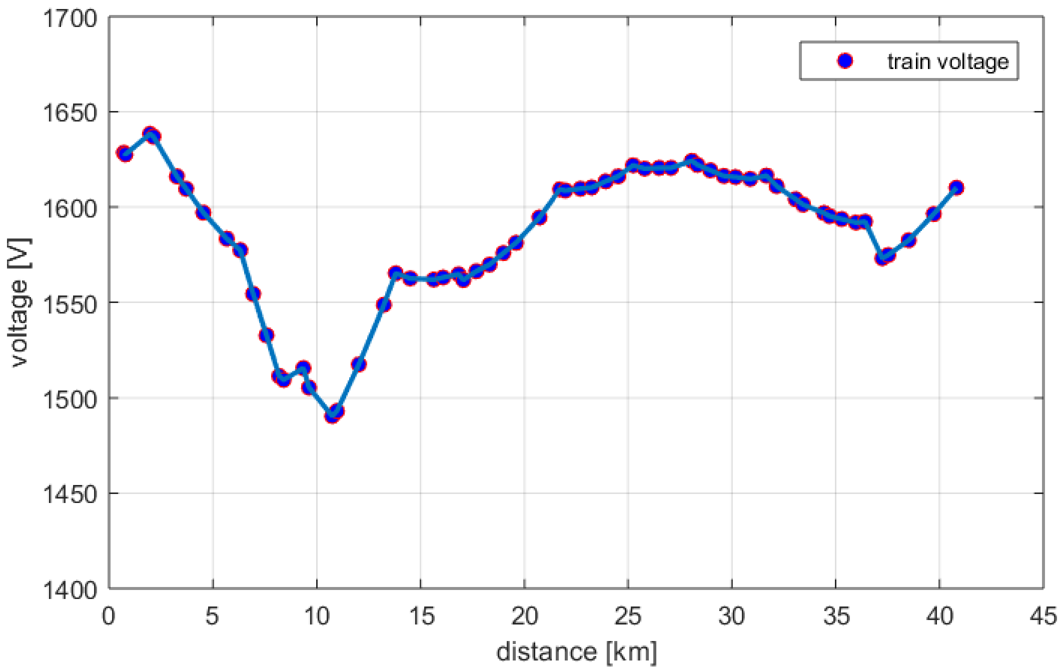

Figure 6-26. Train voltages with a headway of 120s

Figure 6-11 illustrates the output voltage, current and power of the 11 TPSS on the line. The loading factor is each TPSS is between 9.4% and 98%. This is compatible with normal traction systems, as redundancy is necessary to run a full timetable even when one substation is completely out of service.

Table 6-11. Instantaneous quantities for the TPSS

No.	Location [m]	Voltage [V]	Current [A]	Power [kW]
1	0	1614	1050	1733
2	2092	1637	376	620
3	6320	1577	2130	3515
4	9374	1516	3927	6479
5	13798	1565	2488	4105
6	16869	1566	2469	4074
7	21712	1609	1194	1971
8	25247	1622	825	1362
9	28078	1624	756	1248
10	31664	1616	984	1624
11	36412	1592	1692	2792

Table 6-12 shows the main quantities of all the trains travelling on the line. In this table, the direction is up for 0 and down for 1. Also, the meaning of operating mode is 0 for normal, 1 for overvoltage and 2 for undervoltage. The table confirms that all the trains are running normally, as the voltage of the line is within the limits. This is also confirmed by the fact that the trains draw an actual power equal to their power demand, i.e. the power necessary to follow the desired speed diagram.

The specific operating conditions of the trains is variable as expected from normal operations. The trains drawing a large amount of current are accelerating; the trains drawing a small amount of current are coasting or braking with dissipative braking (on-board rheostats); and the train drawing a negative power are braking with regenerative braking. The voltage level follows the current drawn by the trains. Trains accelerating show the lowest voltage levels and train decelerating show the highest voltage levels. In this situation, all the braking trains regenerate power to other trains, as none of them reaches the threshold for activating the braking rheostats.

Table 6-12. Instantaneous quantities for the trains on the line

No.	Location [m]	Direction	Operating mode	Voltage [V]	Current [A]	Power demand [kW]	Actual Power [kW]
1	714	0	0	1628	-1010	-1644	-1644
2	790	1	0	1628	189	308	308
3	1974	0	0	1638	-1003	-1644	-1644
4	2137	1	0	1637	-632	-1035	-1035
5	3267	0	0	1616	190	308	308
6	3714	1	0	1610	57	92	92
7	4538	0	0	1597	193	308	308
8	5667	1	0	1583	194	308	308
9	6319	0	0	1577	59	93	93
10	6938	1	0	1554	198	308	308
11	7578	0	0	1533	61	94	94
12	8190	1	0	1512	1647	2490	2490
13	8405	0	0	1509	1377	2079	2079
14	9353	1	0	1516	745	1129	1129
15	9625	0	0	1505	1654	2490	2490
16	10742	1	0	1491	1671	2490	2490
17	10969	0	0	1493	1183	1767	1767
18	12024	1	0	1518	203	308	308
19	13229	0	0	1549	199	308	308
20	13798	1	0	1565	59	93	93
21	14500	0	0	1563	197	308	308
22	15629	1	0	1562	197	308	308
23	16077	0	0	1563	61	96	96
24	16820	1	0	1565	1075	1682	1682
25	17052	0	0	1562	1594	2490	2490
26	17681	1	0	1566	60	94	94
27	18315	0	0	1570	196	308	308
28	18979	1	0	1576	60	94	94
29	19586	0	0	1581	195	308	308
30	20714	1	0	1594	193	308	308
31	21710	0	0	1609	-27	-43	-43
32	21986	1	0	1609	191	308	308

33	22713	0	0	1610	58	93	93
34	23257	1	0	1610	191	308	308
35	23930	0	0	1613	58	93	93
36	24529	1	0	1616	190	308	308
37	25247	0	0	1622	57	93	93
38	25800	1	0	1620	190	308	308
39	26504	0	0	1621	57	93	93
40	27072	1	0	1621	190	308	308
41	28076	0	0	1624	-57	-92	-92
42	28343	1	0	1622	190	308	308
43	28968	0	0	1619	58	94	94
44	29615	1	0	1616	190	308	308
45	30176	0	0	1616	58	94	94
46	30886	1	0	1615	191	308	308
47	31664	0	0	1616	57	92	92
48	32158	1	0	1611	191	308	308
49	33072	0	0	1604	57	91	91
50	33429	1	0	1601	192	308	308
51	34435	0	0	1597	-64	-102	-102
52	34700	1	0	1595	193	308	308
53	35286	0	0	1594	59	94	94
54	35972	1	0	1592	193	308	308
55	36411	0	0	1592	60	96	96
56	37243	1	0	1573	1583	2490	2490
57	37522	0	0	1575	668	1053	1053
58	38515	1	0	1583	195	308	308
59	39720	0	0	1596	193	308	308
60	40811	1	0	1610	1467	2361	2361

6.2.4 Power analysis of TPSS

This section investigates in more details the power of the TPSS and the impact on the presence of an additional converter enabling energy regeneration to the distribution grid. The analysis has been repeated for different headways, as they affect the average power consumption and losses on the electrification system and the substations.

6.2.4.1 Headway of 120 s

Substation results

Figure 6-27 and Figure 6-28 show the power of each substation during a time interval equal to the headway (120 s), this is because these diagrams are periodic of the headway time at steady-state. The instantaneous power of the TPSS is significantly variable due to the different operating conditions of the trains and the different position on the line. Additionally, the power of all TPSS is always positive, as diodes do not allow any regenerative braking back to the 15 kV power distribution grid.

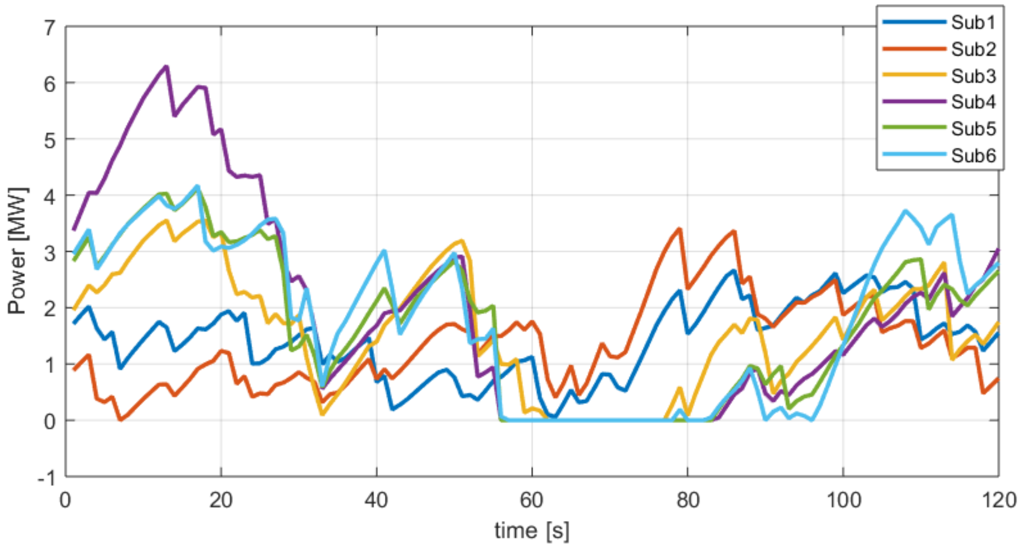

Figure 6-27. Power of each traction substation

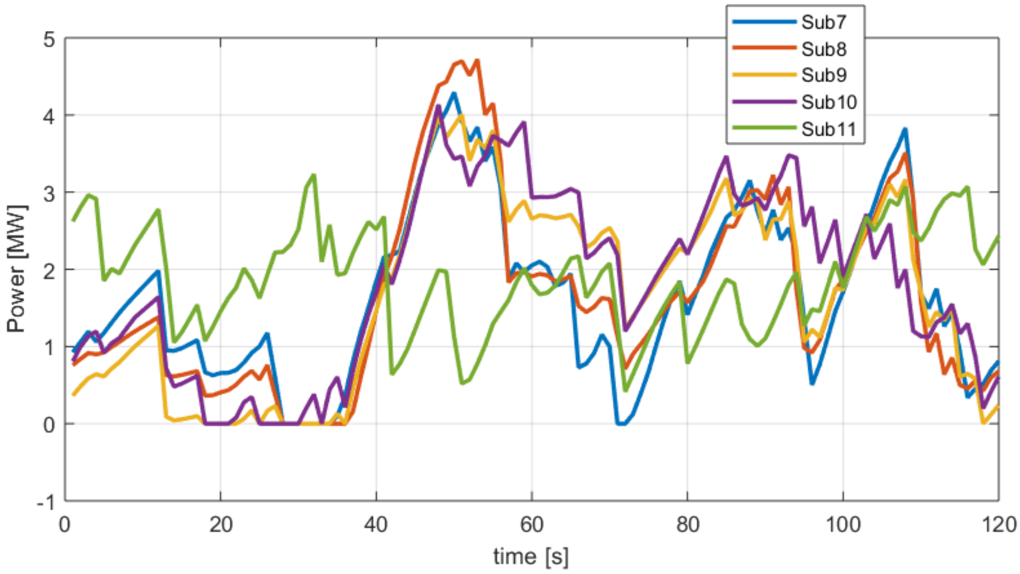

Figure 6-28. Power of each traction substation

In order to compare better the actual loading of TPSS, Table 6-4 shows the maximum, minimum and average power of each substation. All the substations have some instants where do not supply any power or only supply very low power to the trains. This is normal for DC traction system, as trains are powered mainly by the two adjacent substations.

Table 6-4 also shows that the maximum power is several times higher the average power, with factors between 172% and 319%. No instantaneous power of TPSS exceeds the rated power, although this is acceptable for a short period. For comparison, in the UK typical duty classes of TPSS are class F (120% overloading for 60 minutes, 150% for 5 minutes and 300% for 1 minute) class G (177.5% for 60 minutes, 283% for 5 minutes and 382.9% for 1 minute) and class H (100% for 60 minutes, 150% for 1 minute).

Table 6-13 Maximum, minimum and average power of each TPSS

No.	Maximum power [MW]	Minimum power [MW]	Average power [MW]
1	2.66	0.06	1.42
2	3.41	0.00	1.36
3	3.55	0.00	1.59
4	6.30	0.00	1.97
5	4.12	0.00	1.69
6	4.17	0.00	1.80
7	4.29	0.00	1.66
8	4.72	0.00	1.66
9	4.01	0.00	1.67
10	4.13	0.00	1.85
11	3.23	0.42	1.88

Figure 6-29 and Figure 6-30 describe the voltage of each TPSS over the time. The voltage ranges from 1512 to 1830 V.

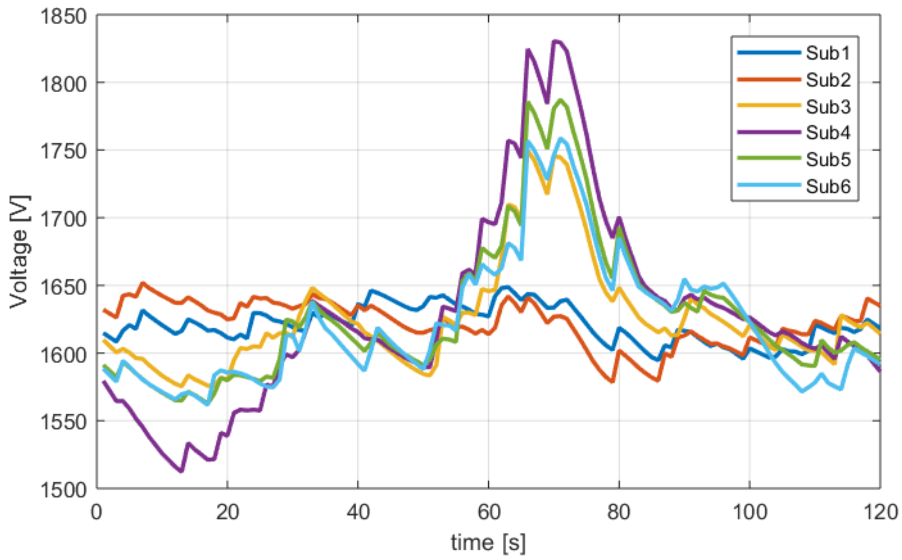

Figure 6-29 Voltage of each traction substation

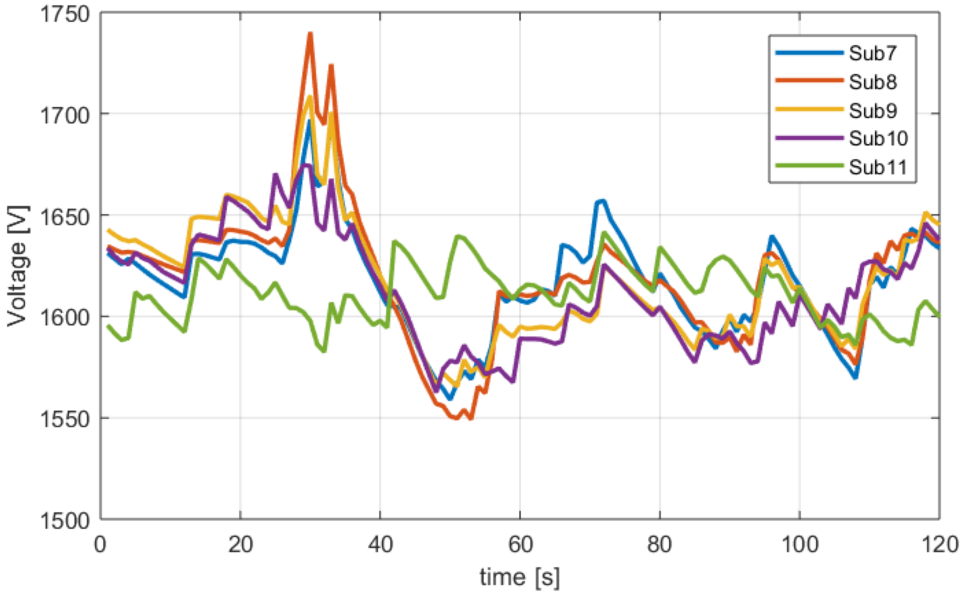

Figure 6-30 Voltage of each traction substation

Train results

The power and voltage profiles of train on the up and down tracks are shown in Figure 6-31 and Figure 6-32. For the train on the up track, the voltage is between 1489 and 1834 V. The train travels for 3605 s. The total duration of overvoltage (voltage > 1800 V) is 24 s, which accounts for 0.67% of the total journey time. The period of using braking resistance is short.

For the train on the down track, the voltage is between 1486 and 1834 V. The train travels for 3550 s. The total duration of overvoltage (voltage > 1800 V) is 19 s, which accounts for 0.54% of the total journey time. The period of using braking resistance is short.

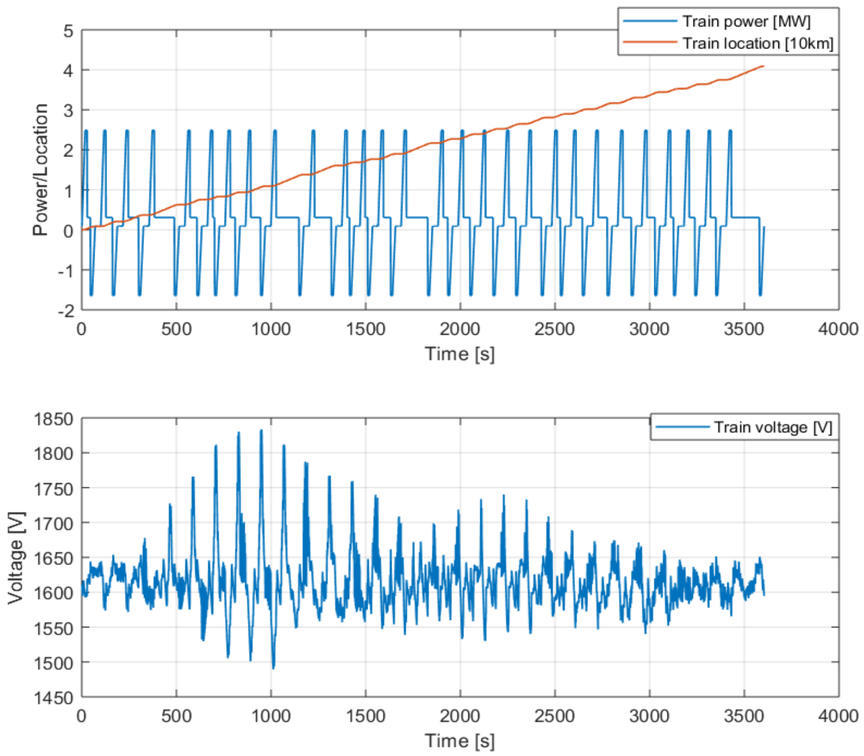

Figure 6-31 Power and voltage profile of a train travelling from Puerta del Sur to Parque Lisboa (up)

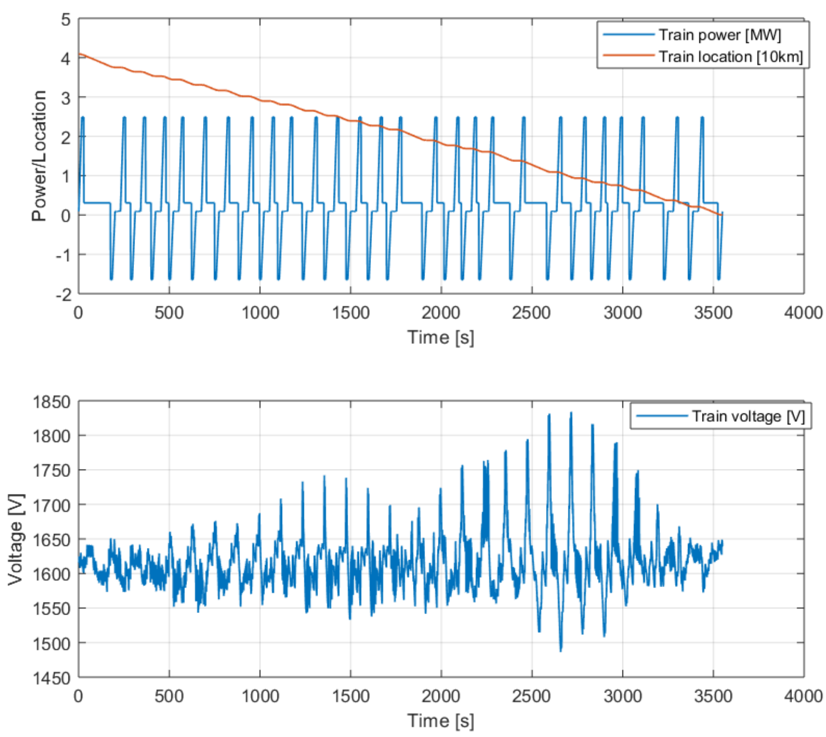

Figure 6-32 Power and voltage profile of a train travelling from Puerta del Sur to San Nicasio (down)

Reversible substation results

The energy consumption has been recalculated when one of the TPSS is reversible for the presence of the sSOP, as shown in Table 6-5. The number 0 means that no TPSS are reversible (baseline case), whereas 1 means that TPSS 1 is reversible and so on. Table 6-5 shows that when the sSOP is located at TPSS 4 the line achieves the lowest energy consumption. With the introduction of one sSOP, the efficiency of regeneration is improved for all the configurations.

However, the energy-saving performance of using sSOP is not significant. This is because the regeneration efficiency without sSOP when headway is 120 s is very high, nearly 100%.

Table 6-14 Energy consumption with a sSOP installed at one of the TPSS

Location of the sSOP		0	1	2	3	4	5	6	7	8	9	10	11
Headway	[s]	120	120	120	120	120	120	120	120	120	120	120	120
E_s	kWh	618	618	618	618	617	618	618	618	618	618	618	618
$E_{s,rectified}$	kWh	618	618	618	620	623	621	620	618	618	618	618	618
$E_{s,inverted}$	kWh	0.0	0.0	0.0	-1.7	-6.0	-3.1	-2.0	0.0	-0.4	0.0	0.0	0.0
$E_{s,loss}$	kWh	18.5	18.5	18.5	18.7	19.0	18.8	18.7	18.5	18.6	18.5	18.5	18.5
$E_{t,loss}$	kWh	12.5	12.5	12.5	12.4	11.6	12.2	12.3	12.5	12.5	12.5	12.5	12.5
$E_{traction,demand}$	kWh	861	861	861	861	861	861	861	861	861	861	861	861
$E_{traction}$	kWh	861	861	861	861	861	861	861	861	861	861	861	861
$E_{braking,available}$	kWh	453	453	453	453	453	453	453	453	453	453	453	453
$E_{braking}$	kWh	453	453	453	453	453	453	453	453	453	453	453	453
η_{regen}	%	100%	100%	100%	100%	100%	100%	100%	100%	100%	100%	100%	100%

Figure 6-6 and Figure 6-34 describe how the power curves of TPSS are affected for the presence of one sSOP at TPSS 4. The regenerative power of the sSOP depends on the control scheme of the power converter. In this simulation, there is a fixed linear voltage regulation characteristic for the converter. The analysis shows that the maximum regenerative power of the sSOP at TPSS 4 is around 2 MW.

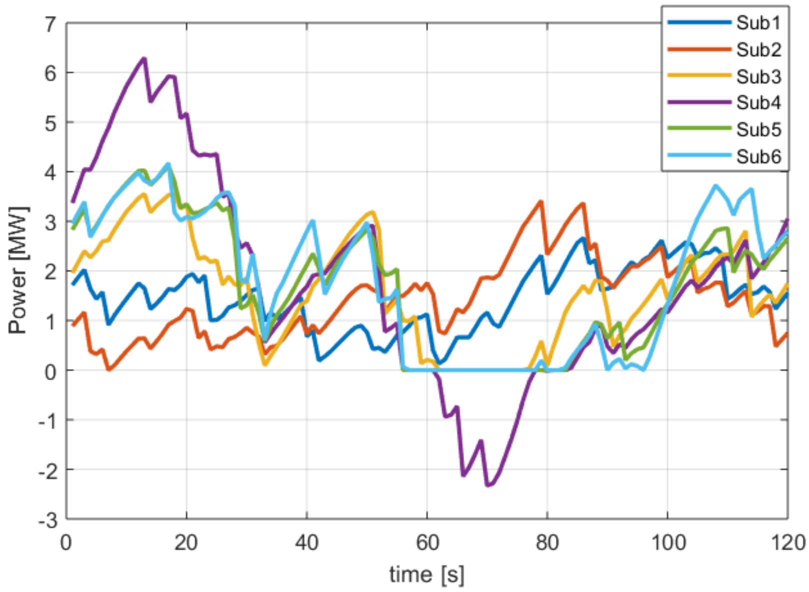

Figure 6-33. Instantaneous power of TPSS when sSOP is at TPSS 4

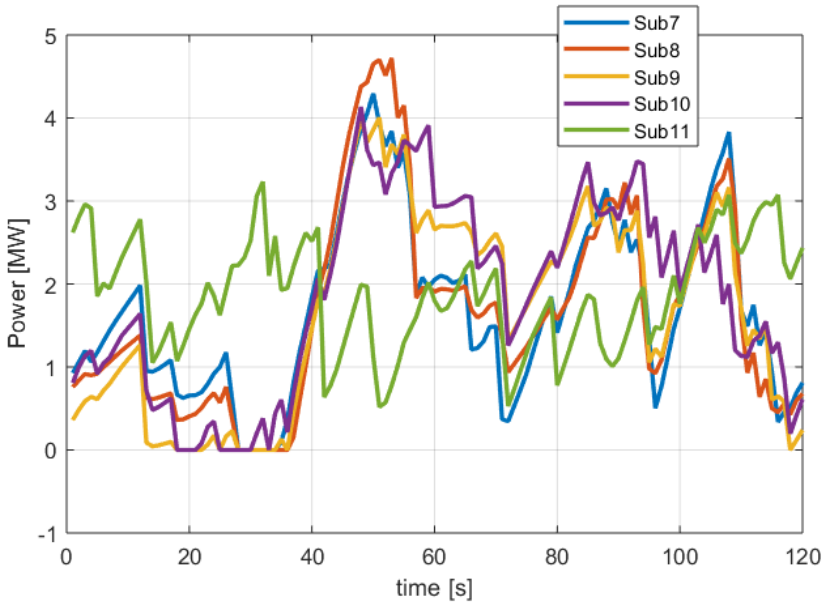

Figure 6-34. Instantaneous power of TPSS when sSOP is at TPSS 4

6.2.4.2 Headway of 660 s

Substation results

Figure 6-35 and Figure 6-36 show the power of each substation during a time interval equal to the headway (660 s), this is because these diagrams are periodic of the headway time at steady-state. The instantaneous power of the TPSS is significantly variable due to the different operating conditions of the trains and the different position on the line. Additionally, the power of all TPSS is always positive, as diodes do not allow any regenerative braking back to the 15 kV power distribution grid.

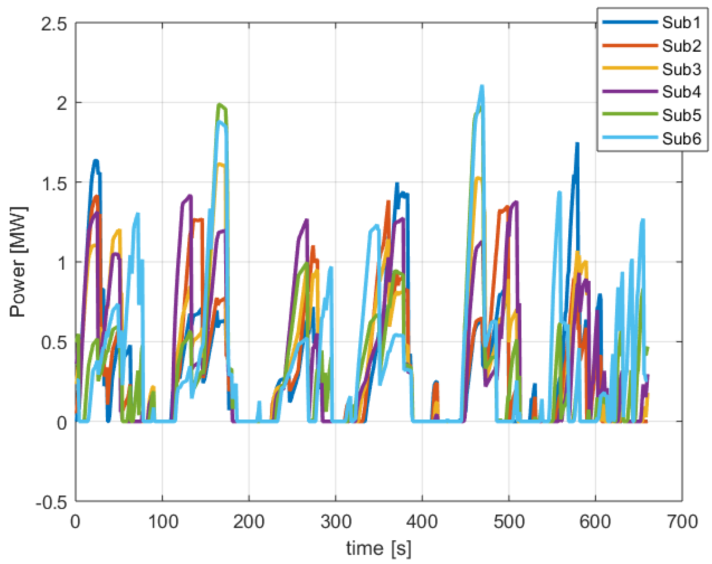

Figure 6-35. Power of each traction substation

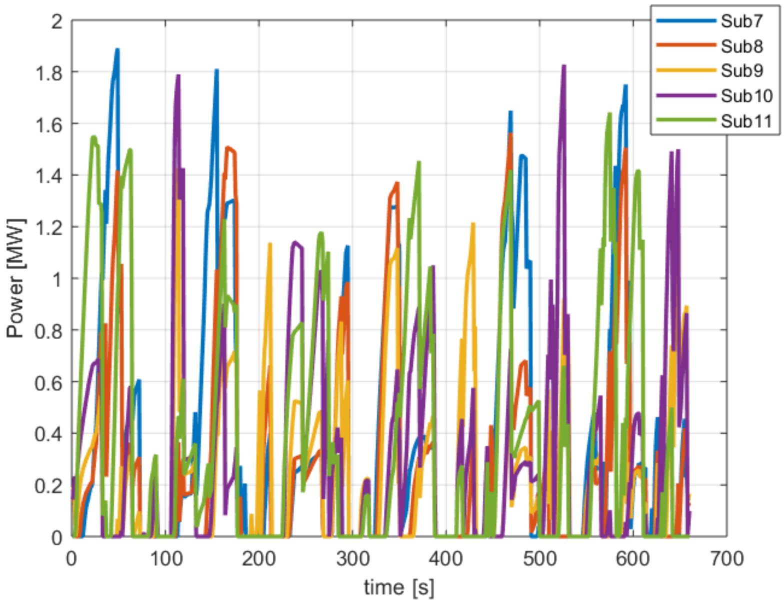

Figure 6-36. Power of each traction substation

In order to compare better the actual loading of TPSS, Table 6-15 shows the maximum, minimum and average power of each substation. All the substations have some instants where do not supply any power or only supply very low power to the trains. This is normal for DC traction system, as trains are powered mainly by the two adjacent substations.

Table 6-15 also shows that the maximum power is several times higher the average power, with factors between 381% and 628%. No instantaneous power of TPSS exceeds the rated power, although this is acceptable for a short period. Both the maximum power and average power are lower than those when headway is 120 s.

Table 6-15 Maximum, minimum and average power of each TPSS

No.	Maximum power [MW]	Minimum power [MW]	Average power [MW]
1	1.75	0.00	0.31
2	1.42	0.00	0.33
3	1.61	0.00	0.37
4	1.42	0.00	0.37
5	1.99	0.00	0.32
6	2.11	0.00	0.37
7	1.89	0.00	0.38
8	1.56	0.00	0.30
9	1.43	0.00	0.25
10	1.83	0.00	0.30
11	1.64	0.00	0.39

Figure 6-37 and Figure 6-38 describe the voltage of each TPSS over the time. The voltage ranges from 1607 to 1892 V. The voltage is higher than the voltage when headway is 120 s.

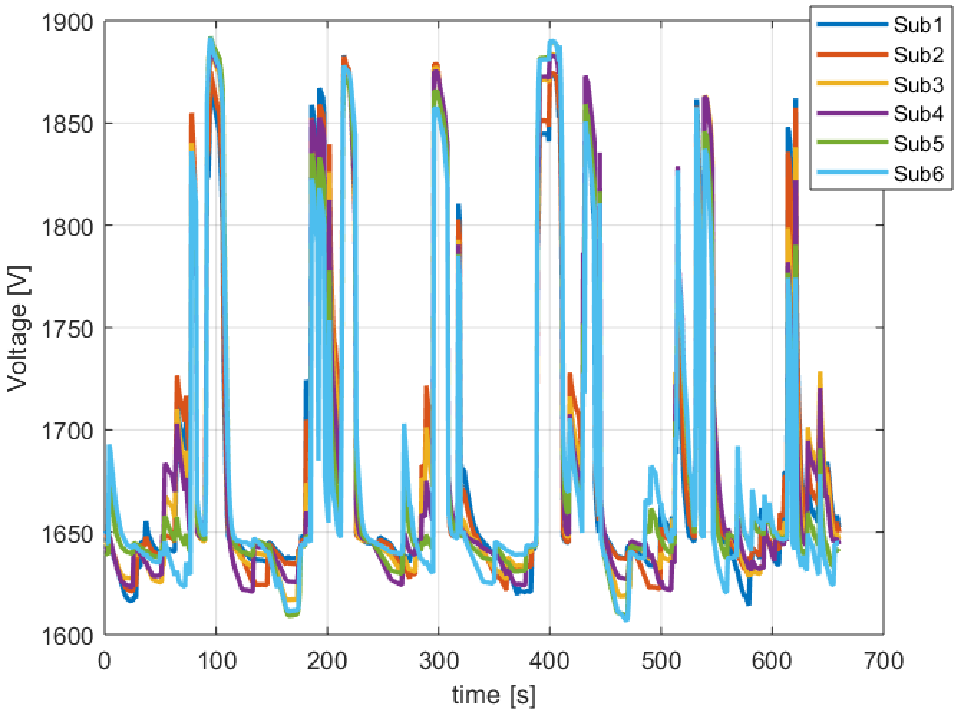

Figure 6-37 Voltage of each traction substation

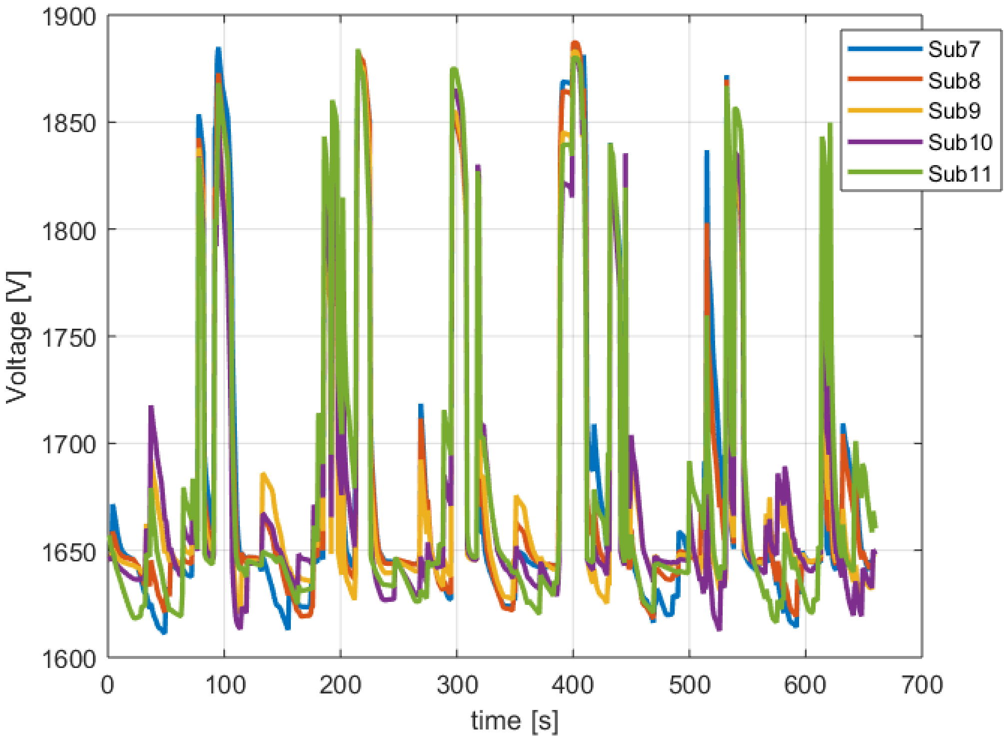

Figure 6-38 Voltage of each traction substation

Train results

The power and voltage profiles of train on the up and down tracks are shown in Figure 6-39 and Figure 6-40. For the train on the up track, the voltage is between 1588 and 1892 V. The train travels for 3605 s. The total duration of overvoltage (voltage > 1800 V) is 507 s, which accounts for 14% of the total journey time.

For the train on the down track, the voltage is between 1586 and 1893 V. The train travels for 3550 s. The total duration of overvoltage (voltage > 1800 V) is 515 s, which accounts for 15% of the total journey time.

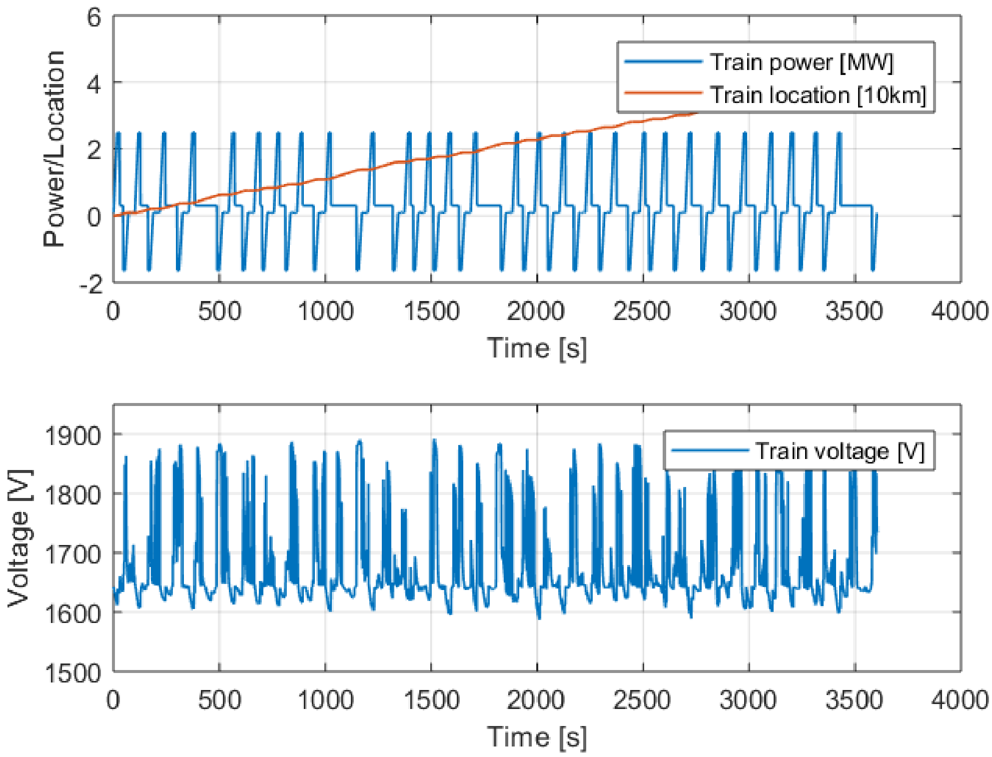

Figure 6-39 Power and voltage profile of a train travelling from Puerta del Sur to Parque Lisboa (up)

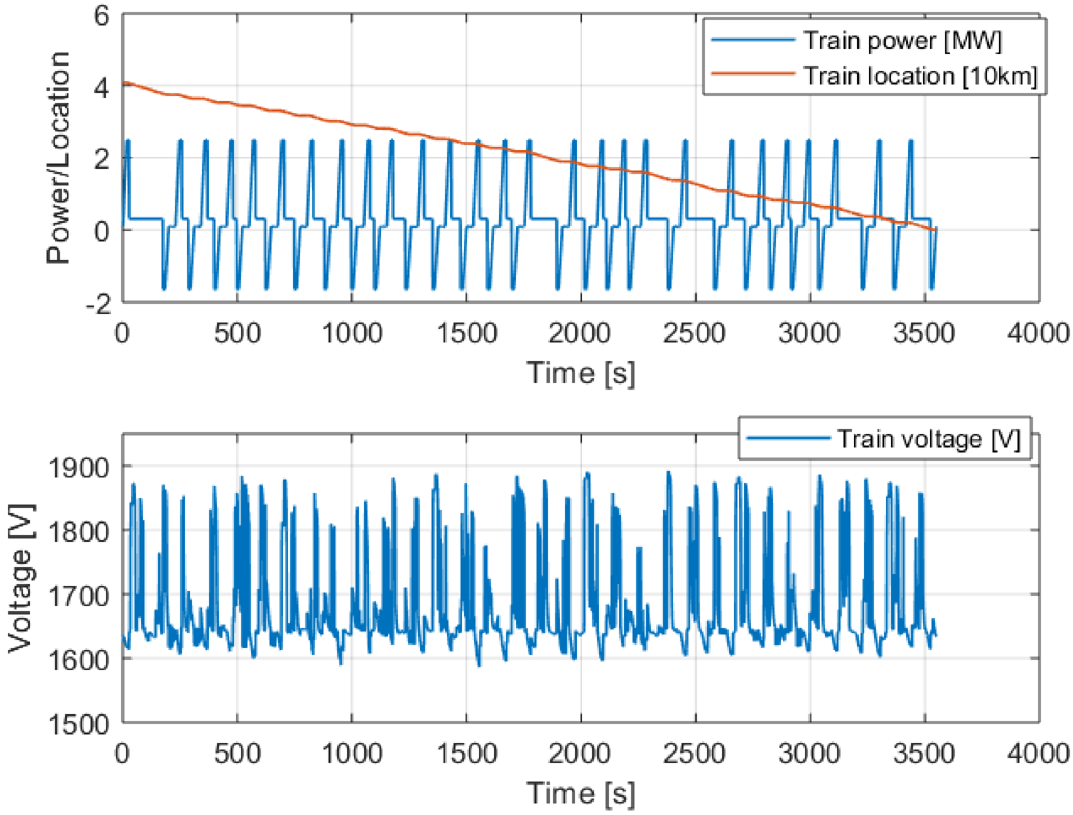

Figure 6-40 Power and voltage profile of a train travelling from Puerta del Sur to San Nicasio (down)

Reversible substation results

The energy consumption has been recalculated when one of the TPSS is reversible for the presence of the sSOP, as shown in Table 6-16. The number 0 means that no TPSS are reversible (baseline case), whereas 1 means that TPSS 1 is reversible and so on. Table 6-16 shows that when the sSOP is located at TPSS 5 and TPSS 6, the line achieves the lowest energy consumption. With the introduction of one sSOP, the efficiency of regeneration is improved for all the configurations. The energy-saving performance of using sSOP reduces the energy consumption up to 7%.

Table 6-16: Energy consumption with a sSOP installed at one of the TPSS

Location of the sSOP		0	1	2	3	4	5	6	7	8	9	10	11
Headway	[s]	660	660	660	660	660	660	660	660	660	660	660	660
E_s	kWh	675	639	638	634	632	628	628	634	637	641	643	641
$E_{s,rectified}$	kWh	675	679	680	679	679	678	678	678	676	675	676	677
$E_{s,inverted}$	kWh	0	-40	-42	-45	-47	-50	-49	-44	-40	-35	-33	-37
$E_{s,loss}$	kWh	20.3	22.5	22.6	22.8	22.8	23.0	22.9	22.7	22.4	22.1	22.0	22.3
$E_{t,loss}$	kWh	13.9	15.6	15.5	15.2	15.3	15.2	15.3	15.9	16.1	16.4	16.3	15.9
$E_{traction,demand}$	kWh	861	861	861	861	861	861	861	861	861	861	861	861
$E_{traction}$	kWh	861	861	861	861	861	861	861	861	861	861	861	861
$E_{braking,available}$	kWh	453	453	453	453	453	453	453	453	453	453	453	453
$E_{braking}$	kWh	399	438	440	444	446	450	450	445	442	438	435	437
η_{regen}	%	88%	97%	97%	98%	98%	99%	99%	98%	98%	97%	96%	97%

Figure 6-41 and Figure 6-42 describe how the power curves of TPSS are affected for the presence of one sSOP at TPSS 5. The regenerative power of the sSOP depends on the control scheme of the power converter. In this simulation, there is a fixed linear voltage regulation characteristic for the converter. The analysis shows that the maximum regenerative power of the sSOP at TPSS 5 is around 4.2 MW.

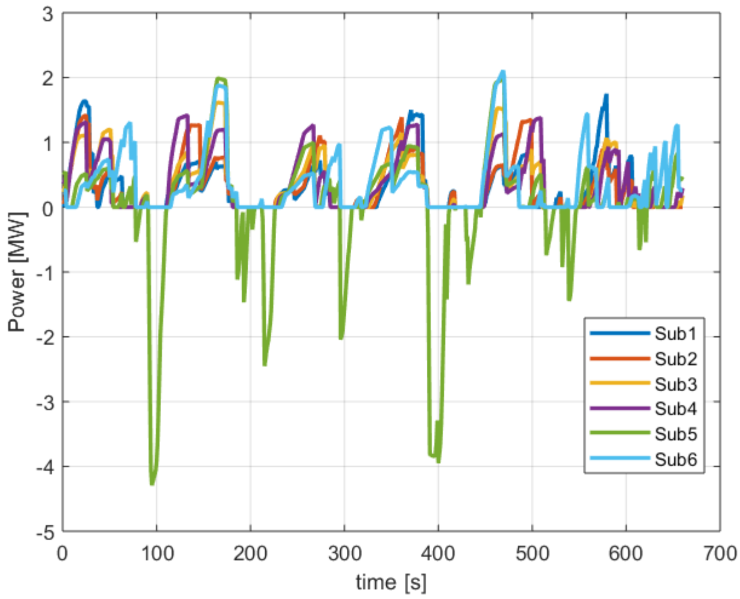

Figure 6-41. Instantaneous power of TPSS when sSOP is at TPSS 4

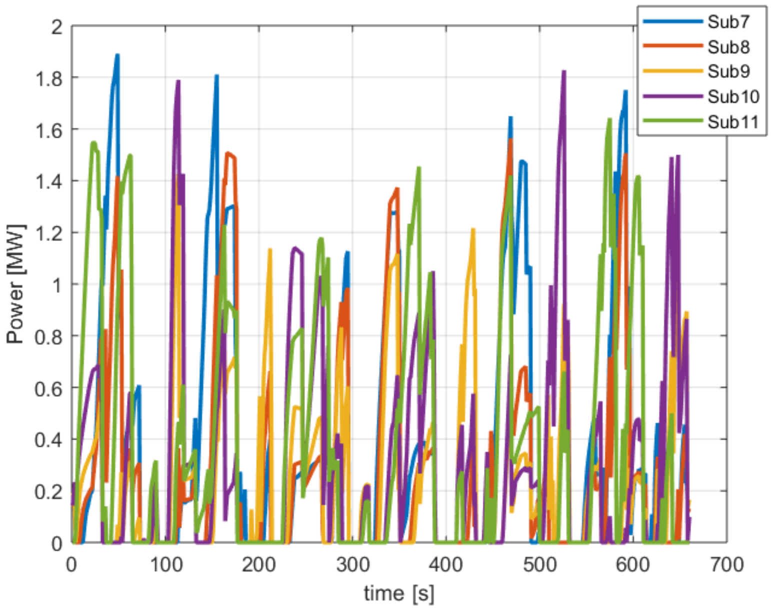

Figure 6-42. Instantaneous power of TPSS when sSOP is at TPSS 4

7 Analysis of the approaches to prevent energy losses

7.1 Driving style optimisation

The train speed profile is determined by train driving controls, which is a key factor influencing the traction energy consumption. An example of three speed profiles with different driving styles is given in Figure 7-1. Speed profile 1 accelerates to a highest speed with a longer coasting pattern, while speed profile 2 accelerates to a medium speed with a shorter coasting pattern. Speed profile 3 accelerates to a lowest speed and remains this speed until braking. There is a large amount of literature studying the impact on energy consumption of different driving controls. Compared with flat-out driving, driving with coasting controls can reduce the energy consumption by about 30% with a 5% increase in journey time.

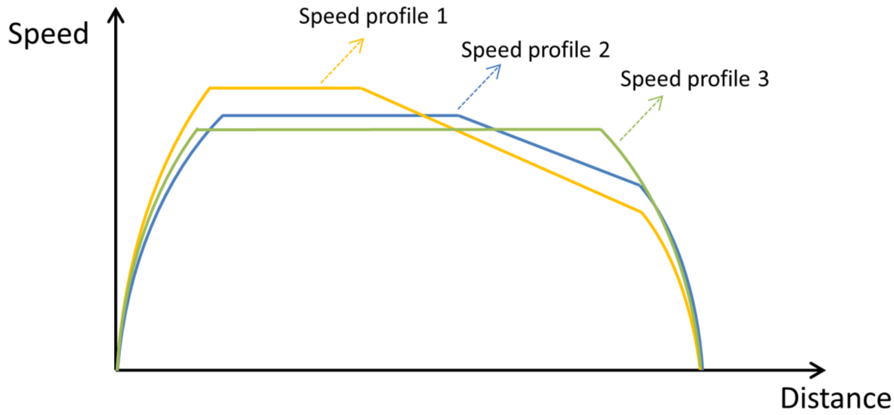

Figure 7-1 Examples of various speed profiles

An applicable driving solution for reducing traction energy consumption was employed in Edinburgh Tram[15]. The theoretical optimal driving strategies are produced by train simulation using an enhanced Brute Force searching algorithm. In order to achieve the application of energy-efficient strategies, a DPTS (Driver Practical Training System) was developed and coasting signage was tested by Edinburgh Tram. Compared with normal driving, driving with the DPTS reduced the traction energy consumption by around 15%, where the timetable is the same. Driving with coasting signage is easy to install and simple for human drivers to practice. The field test indicates that the traction energy of driving with coasting signage is reduced by around 10%, where a shorter journey time is achieved. From the field test, it can be concluded that with practice the driver can improve the energy saving performance.

7.2 Timetable scheduling

In modern railway systems with regenerative braking implemented, motoring trains collect electricity from substations and trains in regenerative braking. When the train is braking, motors transform mechanical energy available at the drive shaft into electrical energy. Then, the electrical energy is transferred back to the network system to power other trains in traction. For normal

[15] Z. Tian, N. Zhao, S. Hillmansen, C. Roberts, T. Dowens, and C. Kerr, "SmartDrive: Traction Energy Optimization and Applications in Rail Systems," IEEE Transactions on Intelligent Transportation Systems (Early Access), DOI: 10.1109/TITS.2019.2897279, 2019.

regenerative braking, all of the regenerating energy can be transferred into the transmission network to power other trains. However, as regenerative braking can increase the voltage of a train, a high regen voltage will occur when there are not enough motoring trains absorbing the regenerative energy in the power network. In case of a high voltage hazard, some braking energy is prevented from transferring into contact lines. This part of the braking energy is wasted in the on-board braking rheostat as heat until the network voltage is below the safe value. Based on a DC 1500 V metro line in Korea, the reused regenerative braking energy was calculated based on the measurement of catenary voltage and current, where around 21-39% of traction energy was reused due to regenerated braking[16]. Therefore, it is essential to analyse and improve the amount of usable regenerative energy in railways.

The current strategies for improving regenerative braking energy in urban rails include timetable and trajectory optimisation as well as the implementation of energy storage systems (ESS) and reversible substations[17]. Optimising braking trajectory and timetable can improving the efficiency of using regenerative energy. The Bellman-Ford algorithm was implemented in the optimisation of braking speed trajectory. The regenerative braking energy then increased by 17.23%[18]. The usage of regenerative braking energy can be improved by synchronising the braking phase with the accelerating phase of trains running in the same power network[19]. Figure 7-2 illustrate the power synchronisation of two trains.

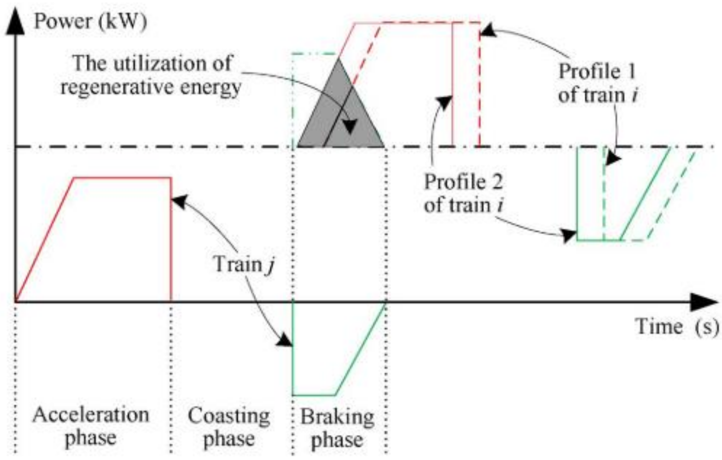

Figure 7-2 Illustration of power-time profiles of two trains [20]

A mathematical programming optimisation model was developed to optimise the synchronisation where a power flow model of the electrical network was used for validation. The optimised timetable improves the energy savings by 7%, without having any effect on the current quality of passenger flow.

[16] B. Chang-han, J. Dong-uk, K. Yong-gi, C. Se-ky, and M. Jai-kyun, "Calculation of regenerative energy in DC 1500V electric railway substations," in 2007 7th Internatonal Conference on Power Electronics, 2007, pp. 801-805.

[17] A. González-Gil, R. Palacin, and P. Batty, "Sustainable urban rail systems: Strategies and technologies for optimal management of regenerative braking energy," Energy Conversion and Management, vol. 75, pp. 374-388, 2013.

[18] S. Lu, P. Weston, S. Hillmansen, H. B. Gooi, and C. Roberts, "Increasing the Regenerative Braking Energy for Railway Vehicles," IEEE Transactions on Intelligent Transportation Systems, vol. 15, pp. 2506-2515, 2014.

[19] A. Nasri, M. F. Moghadam, and H. Mokhtari, "Timetable optimization for maximum usage of regenerative energy of braking in electrical railway systems," in SPEEDAM 2010, 2010, pp. 1218-1221.

[20] X. Yang, X. Li, B. Ning, and T. Tang, "A Survey on Energy-Efficient Train Operation for Urban Rail Transit," IEEE Transactions on Intelligent Transportation Systems, vol. 17, no. 1, pp. 2-13, 2016.

A train cooperative scheduling rule to synchronise the accelerating and braking actions of successive trains was proposed. Based on a case study of Beijing Metro, the overlapping time of accelerating and braking was improved by around 22% by designing an optimal timetable using a Genetic Algorithm (GA)[21].

Table 7-1 shows the system energy consumption for three different operating regimes: the current ATO operation; the best identified by minimising the traction energy; and the best found by minimising the substation energy. The current Automatic Train Operation (ATO) system energy consumption is calculated using a power network simulator using the speed profiles measured by the ATO system. The Traction optimisation column in Table 7-1 shows the energy consumption of the system under the traction optimisation but keeping the original timetable. The interstation journey times and dwell times are fixed and only one coasting point is used in each interstation journey. The results show that both traction energy and substation energy can be reduced by 29.9%. With traction optimisation alone, the regenerative efficiency (regenerative energy divided by braking energy) is almost the same as with ATO at 80.6% and 82.1%, respectively. The significant traction energy saving is probably because the motion simulator applies a perfect optimal speed trajectory which is not achieved in real world. Using substation energy optimisation, the traction energy consumption and braking energy is almost the same with the traction energy optimisation results, but the substation energy is reduced by an additional 10%. This is mainly caused by the higher regenerative efficiency which reaches 95.5%.

Table 7-1 Optimisation results comparison[22]

	Current ATO operation	Driving style optimisation	Driving and timetable optimisation
Cycle running time [s]	4281	4281	4248
Substation energy per headway [kWh]	331.28	232.21	203.37
Substation loss per headway (kWh)	12.38	6.41	4.55
Transmission loss per headway [kWh]	26.26	16.60	16.18
Traction energy per headway [kWh]	525.94	372.52	375.12
Braking energy per headway [kWh]	289.51	199.04	201.57
Regenerative energy per headway [kWh]	233.30	163.32	192.48
Efficiency	80.6%	82.1%	95.5%

7.3 Infrastructure upgrading

Infrastructure upgrading methods to reducing energy losses including using energy storage devices, reversible substation, renewable energy sources. Energy storage devices can be used to store regenerative braking for reuse. Using energy storage systems not only increases the efficiency of the usage of regenerative braking energy, but also reduces the peak load demand for busy traffic. The energy storage devices include batteries, flywheels, electric double layer capacitors and hybrid energy

[21] X. Yang, A. Chen, X. Li, B. Ning, and T. Tang, "An energy-efficient scheduling approach to improve the utilization of regenerative energy for metro systems," Transportation Research Part C: Emerging Technologies, vol. 57, pp. 13-29, 2015.

[22] Z. Tian, P. Weston, N. Zhao, S. Hillmansen, C. Roberts, and L. Chen, "System energy optimisation strategies for metros with regeneration," Transportation Research Part C: Emerging Technologies, vol. 75, pp. 120-135, 2017.

storage devices. The capacity and locations of way-side energy storage devices can be optimised to minimise the energy losses. In reversible DC fed systems with inverting substations, the regenerative braking energy can be converted and fed back to AC networks, which increases the network receptivity.

The energy consumption of a typical metro network without and with reversible substations has been studied[23].The substation energy consumption results with different timetables in a non-inverting system are shown in Figure 7-3. When the headway decreases, the regeneration efficiency increases and leads to a low substation consumption. The minimum energy consumption is 10.3 kWh/train-km, while the maximum is 20.6 kWh/train-km. Around 50% of energy can be saved with the highest receptivity.

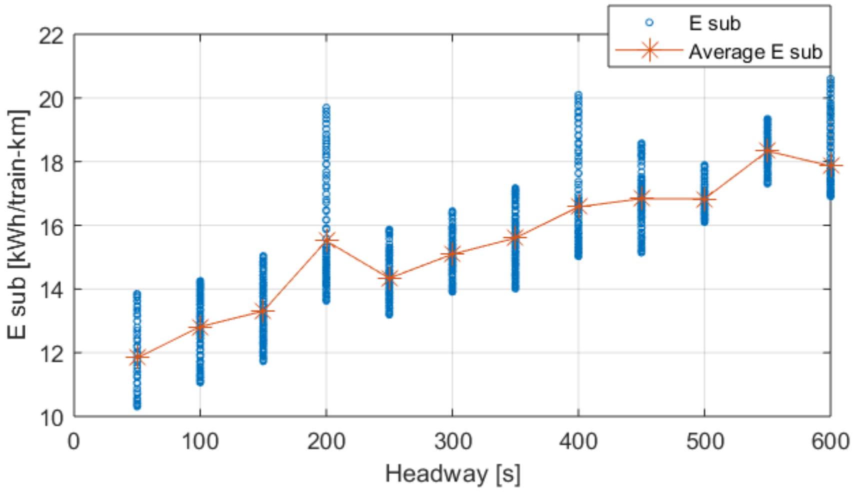

Figure 7-3 Substation energy consumption of a non-inverting system

The substation energy consumption results in an inverting system are shown in Figure 7-4. Although the regeneration efficiency is 100% for an inverting system, the substation energy consumption varies with different timetables. The minimum substation is 10.3 kWh/train-km, which occurs at a headway of 50 s. The maximum substation is 11.2 kWh/train-km, which occurs at a headway of 600 s. The difference between substation energy consumption is mainly because of the difference in transmission losses. The different ratio is not large, which is around 8.7%.

Compared with the energy consumption of the non-inverting system, the percentage of energy saved using inverting substations is shown in Figure 7-5. The energy saving by inverting substations rises with the increase of headway. The saving ratio at a headway of 50 s is between 0 and 0.23, with an average of 0.1. The saving ratio at a headway of 600 s increase to an average of 0.38. By using the inverting substations, the global substation energy consumption could be reduced by around 10-40%.

When a new smart Soft-Open Point (sSOP) device is used to interconnect railway electrification and power distribution networks, the benefit is not only the improvement of the regenerative braking energy usage, but also to support the distribution network from an additional power source. To analyse and optimise the performance of the sSOP, the train operation has to be considered. in the meanwhile, the control strategy of the sSOP should be studied to achieve the best benefit.

---

[23] Z. Tian, G. Zhang, N. Zhao, S. Hillmansen, P. Tricoli, and C. Roberts, "Energy Evaluation for DC Railway Systems with Inverting Substations," in 2018 IEEE International Conference on Electrical Systems for Aircraft, Railway, Ship Propulsion and Road Vehicles & International Transportation Electrification Conference (ESARS-ITEC), 2018, pp. 1-6.

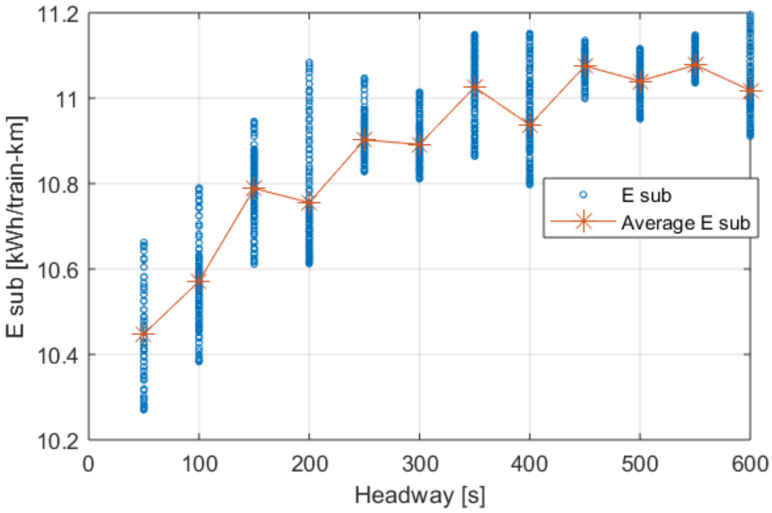

Figure 7-4 Substation energy consumption of an inverting system

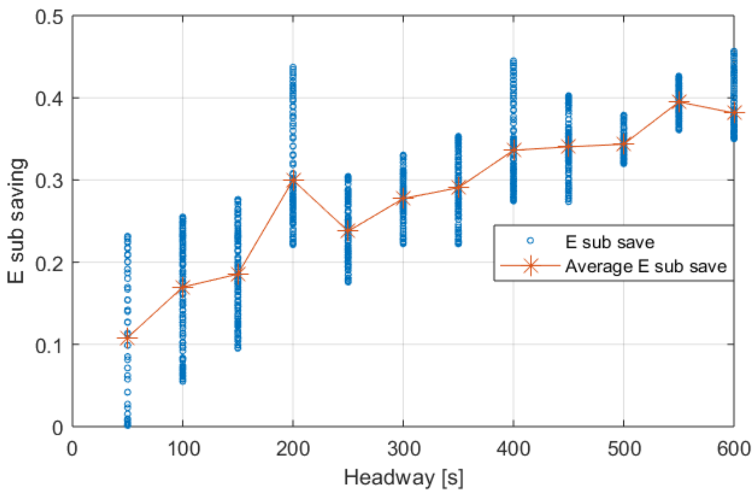

Figure 7-5 Substation energy saving with inverting substations

8 Conclusion

This report has reviewed the feeding arrangement of railway electrical power system. The connection of AC and DC railway and the interface with distribution network are introduced. The energy flow of DC railway systems has been illustrated. The energy losses during the transmission from the distribution network to the trains and from the train braking back to the network have been analysed. The simulation tools to study train movement (driving strategy), timetable and multi-train power flow analysis have been illustrated. Based on the simulation tools, the energy consumption of train auxiliary, traction system, transmission network and substation can be fully studied.

Two metro networks (MDM Line 2 and Line 12) have been studied based on the proposed simulation tool. The power and energy performance of a train driving style with different headways has been evaluated. MDM Line 2 is a straight line, the receptivity of regenerative braking is low when the headway is long. The efficiency of using regenerative braking energy is 65% when the headway is 540 s. However, MDM Line 12, which is a circle line, has a better receptivity of regenerative braking than Line 2. The lowest efficiency of using regenerative braking energy is 88% when the headway is 660 s. Using reversible substations or SOPs can improve the efficiency of using regenerative braking energy to 100%. However, the performance of the improvement depends on the train operation and traction power network arrangement of the existing railway network. Therefore, when upgrading electrical power network, the existing railway network has to be considered and the optimization methods should be developed based on the characteristics of each case.